

# Price Controls Cause Chaos

Brian C. Albrecht\*, Alex Tabarrok<sup>†</sup> and Mark Whitmeyer<sup>‡</sup>

February 7, 2026

---

Price controls kill the incentive for arbitrage. With prices fixed, suppliers become indifferent about where to ship, and allocation depends on parameters that would be economically irrelevant under market clearing. This paper develops a general theory of price controls across multiple markets. We prove a Chaos Theorem: generically, equilibria occur at corners where some markets receive full supply and others receive nothing. Infinitesimal changes in transportation costs, regulatory discretion, or pipeline maintenance can cause discontinuous jumps between these corner solutions. These corner outcomes create an identification problem: welfare depends on valuations at quantities far from the region where demand is locally identified. We therefore introduce a partial-identification approach to welfare that avoids parametric demand extrapolation, prove that sharp welfare bounds are attained by piecewise-linear inverse demands, and reduce computation to a one-dimensional optimization. We illustrate the mechanism in the 1973–74 U.S. gasoline controls. AAA station surveys show that, despite an aggregate shortfall of about 9 percent, rationing was extremely uneven—some states had virtually no sampled stations rationing fuel while others exceeded 90 percent. Applying our bounds implies that misallocation losses can be several times the Harberger triangle, with a benchmark multiple around 3.5×

JEL-Classification: D45, D61, L51, Q41

Keywords: Price controls; Misallocation; Deadweight loss; Market segmentation; Shadow prices; Gasoline shortages

---

\*International Center for Law & Economics. Email: [mail@briancalbrecht.com](mailto:mail@briancalbrecht.com).

<sup>†</sup>George Mason University. Email: [Tabarrok@gmu.edu](mailto:Tabarrok@gmu.edu).

<sup>‡</sup>Arizona State University. Email: [mark.whitmeyer@gmail.com](mailto:mark.whitmeyer@gmail.com).

# 1 Introduction

In February 1974, the aggregate gasoline shortfall was roughly 9 percent nationwide. Price controls on oil kept the price at the pump below the market price. If the standard model of price ceilings held and if markets are similar, each local market would have experienced a roughly proportional 9 percent reduction, shadow prices would equalize, and the Harberger triangle would measure the welfare cost. Instead, pain fell in a patchwork. As Yergin (1991) describes, “gasoline was in short supply in major urban areas, but there were more than abundant supplies in rural and vacation areas, where the only shortage was of tourists.” Why should a 9 percent national shortfall leave some markets with nothing while others have plenty? This paper shows that feast or famine, not modest belt-tightening, is the generic outcome of price controls.

Our formal answer is the Chaos Theorem. When money prices are frozen, suppliers become indifferent about where to ship; any destination earns the same revenue. Allocation then turn on parameters that would be economically irrelevant under market clearing: small differences in transportation costs, regulatory discretion, historical consumption patterns, pipeline maintenance schedules. Cost minimization is a linear program. Linear programs solve at corners. Corners mean some markets get everything, others get nothing. Allocations jump from corner to corner on seemingly trivial changes.

Figure 1 documents this dispersion for the peak of the crisis at the state level, showing the percentage of stations rationing fuel (either completely out of fuel or limiting purchases). Of sampled stations, Connecticut and Massachusetts exceeded 90 percent, while Idaho, Montana, Utah, Hawaii and Wyoming reported no problems. A natural interpretation is that Idaho got lucky and Connecticut got unlucky. But the states with abundant fuel are a sign of the *problem*. Under efficient allocation, a 9 percent national shortfall would translate into a roughly proportional quantity reduction everywhere. The states

Percentage of Stations Rationing Fuel, February 1974

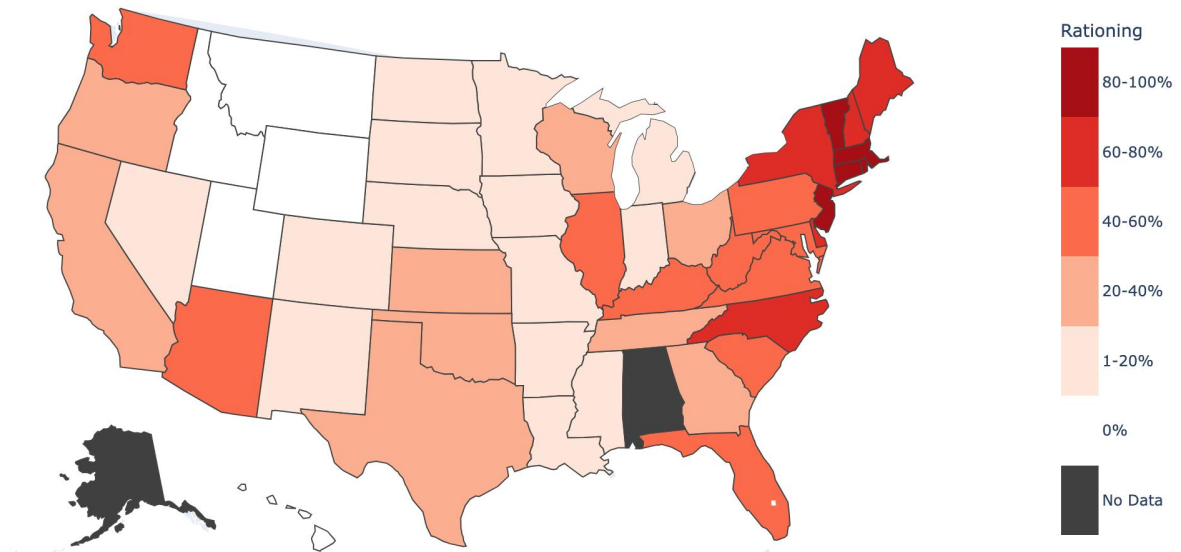


Figure 1: Percentage of gasoline stations rationing fuel by state, February 1974. Rationing includes stations completely out of fuel and those limiting purchases (e.g., maximum gallons per customer). Data are from AAA surveys of sampled stations.

with zero rationing were, in a sense, overserved, since they had enough to satisfy demand even at the controlled price, not just at the market price. At market prices, vacationers in rural areas would never have outbid commuters in cities for scarce fuel. Under a binding ceiling, both pay the same price, so there is no mechanism to redirect supply. The rationing in Connecticut and the abundance in Idaho are two sides of the same misallocation.

This reframes the puzzle. The question is not why some states rationed. With a 9 percent national shortfall, shortages somewhere are inevitable. The question is why other states exhibited no rationing. Why should some markets clear while others run dry? The answer is that efficient allocation requires price variation, which a binding ceiling explicitly forbids. Once prices cannot adjust, there is no mechanism to direct scarce supplies

toward their highest-value uses.

The economic logic is simple. Under market prices, these parameters would matter only at the margin. A slight cost advantage for Pennsylvania over New Jersey would redirect a few tanker loads, not all of them. The price mechanism permits fine-grained reallocation because arbitrageurs capture profits proportional to the price gap they exploit. But when prices are frozen, these incremental profit opportunities vanish. With revenue equalized across destinations, suppliers simply minimize costs. A one-cent cost advantage is as good as a one-dollar advantage; both redirect the entire flow. The economy loses its capacity for incremental adjustment and instead lurches between all-or-nothing extremes (Sowell 1980, p. 137). A refinery outage, a pipeline repair, a regulatory tweak, or any small change in relative costs can flip the entire allocation from one corner to another, with welfare consequences potentially catastrophic even when the triggering parameter change is vanishingly small.

The patchwork pattern of Figure 1 is not an accident. It is the generic outcome when prices cannot signal scarcity.<sup>1</sup>

This corner-solution structure differs from benchmarks in prior work. The Harberger triangle is the *minimum* welfare loss compatible with a binding ceiling and it requires the very price variation a ceiling forbids. Glaeser and Luttmer (2003) quantify misallocation under rent control assuming random allocation, where every apartment has equal probability of reaching any tenant. Random allocation is an interior outcome with its own smoothness: shortages spreads evenly and small parameter changes produce small welfare changes. We show that equilibrium generically occurs at neither the Harberger nor random benchmark. Cost-minimizing suppliers drive allocations to vertices, not interiors (as in Murphy, Shleifer, and Vishny (1992)'s analysis of partial reform). The distinction

1. Pure corner solutions are themselves an extreme case. They assume away contractual rigidities, inventory buffers, and other frictions that slow adjustment. But as a limiting benchmark, corners have empirical bite.

matters: corner solutions where some markets receive nothing generate far larger losses than either efficient or random distributions and those losses jump discontinuously with small parameter perturbations.

The Chaos Theorem creates an identification problem. Under a ceiling, equilibrium allocations are generically corners: some markets clear at the controlled price while others are starved. Welfare depends critically on valuing units at corner allocations. But demand is identified only locally, near the equilibrium point, so welfare accounting requires integrating inverse demand deep into an extrapolation region. Parametric approaches settle that extrapolation by assuming functional form, perhaps bolstered with elasticity sensitivities. We instead ask what welfare statements are possible without committing to a specific extrapolation.

We develop a novel partial-identification framework requiring no parametric demand assumptions. The question becomes: what are the largest and smallest welfare losses consistent with observed allocations and empirically plausible local elasticity restrictions? We prove that both extremes are attained by piecewise-linear inverse demands. The worst case assigns the steepest allowable slope to starved markets and the flattest slope to oversupplied markets, maximizing the shadow price gap. The best case reverses the assignment. Instead of being a robustness check, this is the methodologically appropriate response to a challenge intrinsic to the theoretical contribution.

How large are misallocation losses? We conduct two main exercises. Using station-level survey data from the AAA presented to President Ford during the crisis, our baseline robust interval implies a misallocation-to-Harberger ratio of roughly  $[1.13, 9.06]$ . The quantity reduction accounts for less than one-third of total welfare cost in the benchmark calibration. This exercise pools all open stations against all rationing ones, but we lack pre-crisis station-level data to anchor shadow prices precisely. A second exercise breaks markets up at the state level, where pre-crisis consumption is observed and giving more

to Connecticut means taking from California. Using only state-level variation, the ratio lies in  $[0.26, 2.38]$ , still substantial at the upper end, but state-level data already aggregate within-state misallocation away. Connecticut’s 90 percent rationing becomes a single average quantity, obscuring the gap between open stations in Hartford and closed stations in New Haven.

The remainder of the paper proceeds as follows. Section 2 reviews related literature. Section 3 introduces a two-market example. Section 4 presents the general model. Section 5 develops the Chaos Theorem, and Section 5.4 illustrates the chaos mechanism with simulations. Section 7 applies our framework to the 1973–74 gasoline crisis, developing robust bounds on misallocation losses. We defer proofs to Appendix A and robustness checks using alternative demand specifications to Appendix C.

## 2 Literature Review

Our paper connects three distinct strands of research: the classic welfare-economics treatment of price controls, the modern literature on misallocation, and recent work that uses robust or worst-case methods to bound welfare when key allocation details are unknown.

The canonical approach traces back to Harberger (1954), who measured the efficiency cost of quantity reductions with the familiar “triangle.” Early analyses of price ceilings took the triangle as their primary yardstick. (e.g. Oi (1976), Gordon (1973), and Rockoff (1984) for U.S. wartime experience).

A subsequent literature pointed out that the triangle misses the welfare costs of non-price rationing. Barzel (1974) showed that when money prices are suppressed, rationing by waiting emerges: consumers queue until the shadow “time price” clears the market. Frech and Lee (1987) and Deacon and Sonstelie (1985, 1989) applied this framework to the 1973–74 gasoline crisis, finding that queuing costs alone could exceed the entire rent

transfer from producers to consumers. Frech and Lee (1987) explicitly consider cross-market allocation, analyzing inefficiencies between urban and rural gasoline markets in California. In their framework, optimal rationing by queuing would equalize *time prices* (money price plus waiting cost) across markets. Misallocation occurs when time prices differ: urban consumers faced longer queues than rural consumers, generating welfare losses from the failure to equalize shadow prices. But crucially, their analysis assumes an interior solution: every market receives positive supply, and inefficiency arises from *unequal* shadow prices across locations. Our paper identifies a distinct source of welfare loss that this queuing literature cannot capture. The Chaos Theorem predicts corner solutions where some markets receive literally nothing—an allocative loss that exists even in a hypothetical world with zero queuing costs.

Our paper is most closely related to Davis and Kilian (2011), who study misallocation in the market for natural gas. Brunt (2025) makes a similar pedagogical point, arguing that misallocation losses under price controls are often larger than the quantity-reduction triangle. Murphy, Shleifer, and Vishny (1992) analyze misallocation under partial price liberalization, showing that when some markets are freed while others remain controlled, supply flows to uncontrolled markets until controlled markets are starved. We extend their framework by characterizing the generic structure of equilibrium allocations (corners) and the discontinuous dependence on nuisance parameters.

A foundational question is whether prices or rationing better allocate scarce goods. Weitzman (1977) shows that the answer depends on the joint distribution of needs and income: the price system dominates when wants are dispersed or incomes are equal, while rationing can dominate when needs are uniform but incomes are unequal. The mechanism-design literature formalizes this tradeoff: Condorelli (2013) characterizes when market mechanisms versus non-market mechanisms are optimal, while Akbarpour, Dworczak, and Kominers (2024) show that non-market allocation dominates when willing-

ness to pay is uninformative about the designer’s welfare weights. Kominers and Dworczak (2025) define price gouging as occurring when lowering the price from the market-clearing level would raise utilitarian welfare. Our paper abstracts from redistributive motives, focusing instead on the allocative inefficiency that arises when a binding ceiling segments markets and blocks arbitrage.

Our paper builds on the literature studying random allocation under binding price ceilings. Glaeser and Luttmer (2003) show that apartments do not necessarily flow to their highest-value users under rent control, and they quantify the resulting misallocation under random allocation. Bulow and Klemperer (2012) characterize when consumer surplus rises or falls under different demand-curve shapes.

We focus instead on market segmentation: markets are naturally segmented by geography, by transaction and transport costs, by final use, and by position in the structure of production. We show that equilibrium generically occurs at neither the Harberger benchmark (efficient allocation) nor the Glaeser-Luttmer benchmark (random allocation). Cost-minimizing suppliers drive allocations to vertices, not interiors.

Recent empirical work on rent control, such as Diamond, McQuade, and Qian (2019) on San Francisco or the comprehensive survey by Kholodilin (2024), documents substantial misallocation in housing, though identification of the allocative component remains challenging. Buurma-Olsen et al. (2025) make progress on this front, finding that Dutch public-housing tenants consume units differing 7.5 percent from their efficient allocation. We provide a general theoretical framework that nests these settings as special cases.

Our robust bounds draw on the literature measuring welfare without fully specifying demand. Hausman and Newey (1995) estimate consumer surplus using nonparametric methods; Hausman and Newey (2016) show that with unobserved heterogeneity, welfare is only partially identified. Kremer and Snyder (2018) characterize worst-case deadweight loss, showing it can approach the entire surplus under extreme demand shapes. Kang

and Vasserman (2025) show that familiar functional forms are extremal within canonical demand families. We contribute by applying these methods to misallocation losses across segmented markets, and by showing that the bound-finding problem reduces to a one-dimensional optimization with piecewise-linear extremals.

### 3 Two Market Example

The simplest setting that exhibits misallocation requires just two submarkets. Consider a national market divided into two submarkets with demand functions  $D_1(p)$  and  $D_2(p)$ . A binding price ceiling  $\bar{p}$  creates a total shortage of  $D(\bar{p}) - S(\bar{p})$ , where  $S(p)$  is aggregate supply. We denote total supply under the ceiling as  $\bar{Q} \equiv S(\bar{p})$ . The quantities allocated must sum to this total:  $q_1 + q_2 = \bar{Q}$ . No market can receive more than it demands at the ceiling price, otherwise the market price would fall below the ceiling. This gives upper bounds  $q_1 \leq D_1(\bar{p}) \equiv \bar{q}_1$  and  $q_2 \leq D_2(\bar{p}) \equiv \bar{q}_2$ . Together, these constraints define the feasible set.

Figure 2 illustrates the welfare consequences of different allocations. In Panel A, the shortage is allocated efficiently: shadow prices equalize across markets at  $p^*$ , yielding deadweight losses  $a$  and  $b$  that sum to the national triangle  $c$ . This is the Harberger case. Panel B shows a corner allocation where Market 1 receives its full demand at the controlled price and Market 2 gets whatever is left. The welfare loss is nearly an order of magnitude larger. The Harberger triangle is not an average outcome but the *smallest* welfare cost compatible with a binding ceiling.

Why should we expect corner allocations rather than the efficient interior? Figure 3 shows the geometry. The constraint  $q_1 + q_2 = \bar{Q}$  defines a downward-sloping line; the upper bounds  $q_i \leq \bar{q}_i$  truncate it to a line segment. The endpoints  $E_1$  and  $E_2$  are corner solutions.

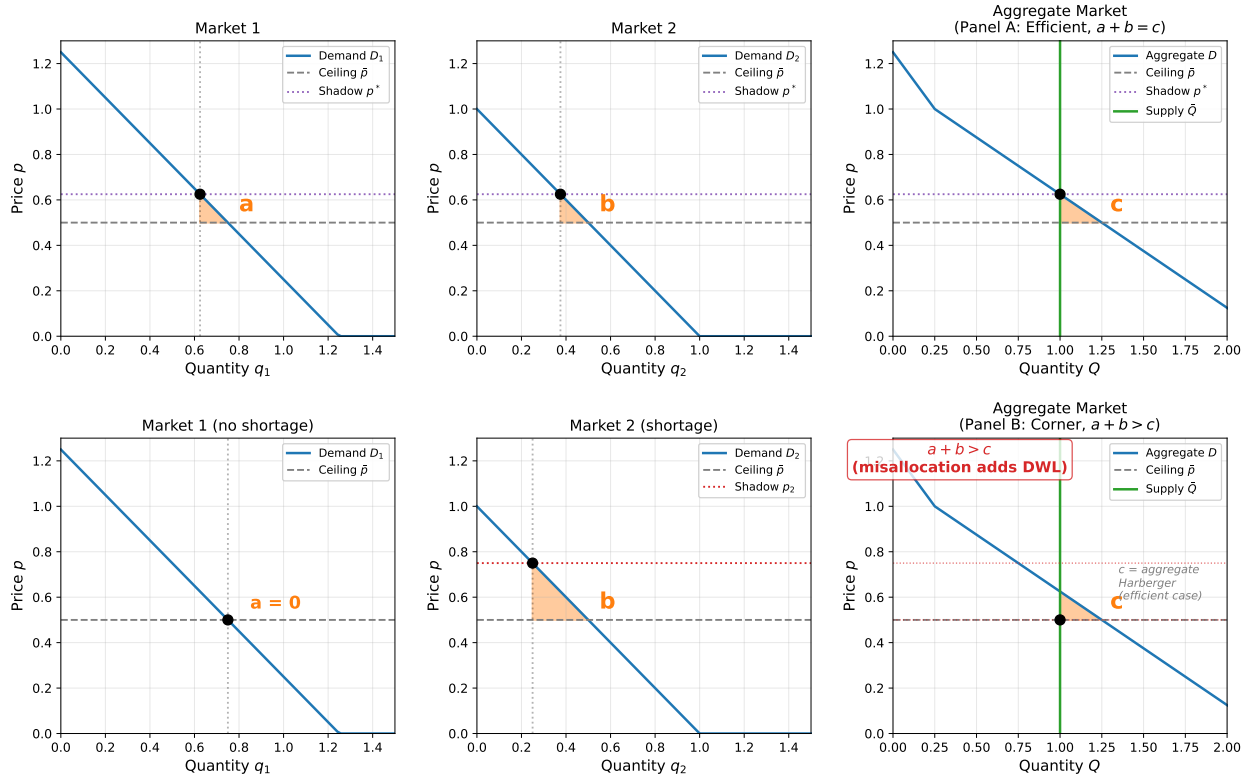


Figure 2: **Two-Market Misallocation under Price Ceiling.** Panel A: efficient allocation with equalized shadow prices;  $a + b = c$ . Panel B: corner allocation where Market 1 receives full demand; shadow prices diverge and  $a + b > c$ .

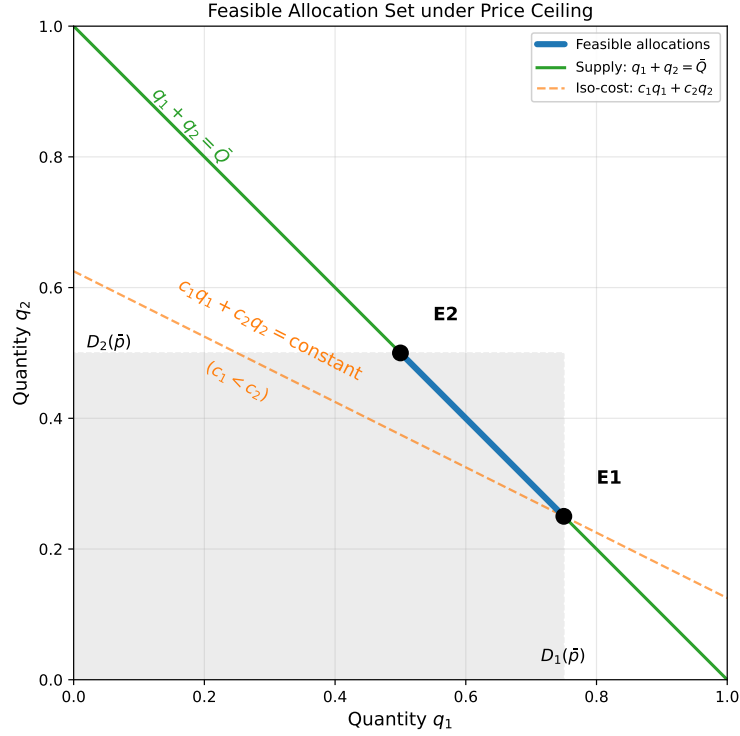


Figure 3: The feasible set is a line segment. Corners  $E_1$  and  $E_2$  are the only generic equilibria under price controls.

Between  $E_1$  and  $E_2$  lies a continuum of feasible allocations. Without price controls, arbitrage would push the economy toward the efficient interior: if gasoline were more valuable in Market 2, traders would profit by redirecting supply until shadow prices equalized. But a binding ceiling eliminates this incentive. With money prices frozen at  $\bar{p}$  everywhere, there is no profit from moving gasoline to where it is more valuable. Sellers are indifferent across all feasible allocations.

This indifference is resolved by any tie-breaking friction. Under normal market conditions, a slight cost advantage would capture only the marginal units; the allocation would adjust incrementally. But with prices frozen, there is no price premium to forgo. Every unit earns identical revenue regardless of destination, so it is possible the entire supply flows to whichever market offers even a fractional cost advantage. Suppose transporting gasoline to Market  $i$  costs  $c_i$  per unit. With prices frozen, suppliers minimize cost. If

$c_1 < c_2$ , supply flows to Market 1; if  $c_2 < c_1$ , it flows to Market 2. The continuum of feasible allocations collapses to a single corner. Interior allocations are generically impossible once  $c_1, c_2 > 0$ . What would have been a marginal reallocation becomes a categorical one. The economy cannot make small adjustments because the price mechanism that would have incentivized them has been disabled.

This corner structure is the source of chaos. When  $c_1$  and  $c_2$  are nearly equal, the economy sits near a knife-edge. A refinery outage, a pipeline repair, a regulatory tweak, any small change in relative costs can flip the entire allocation from  $E_1$  to  $E_2$ . The physical allocation jumps discontinuously even though the underlying parameter change is vanishingly small. And because welfare varies along the feasible set, these discontinuous allocation jumps produce discontinuous welfare jumps.

This is the chaos of price controls. The efficient allocation is a single point in the interior of the feasible set. But equilibrium generically lands at a corner, and which corner depends on incidental details that have nothing to do with consumer valuations. Small perturbations in these incidental details ("nuisance parameters") can flip the economy between corners with sharply different welfare consequences. We formalize this result in [Section 5](#).

While this two-market example clarifies the intuition, a general framework is required to characterize the full range of welfare outcomes. The next section develops such a framework for  $n$  submarkets with general demand functions.

## 4 General Model

We now generalize the two-market example to an arbitrary number of submarkets with general demand functions. The goal is to characterize, for any market structure and any binding price ceiling, the full range of welfare outcomes, from the efficient allocation that

minimizes deadweight loss to the worst-case allocation that maximizes it.

The term 'submarket' is deliberately flexible. Submarkets may be geographic—states, cities, countries—but can also span temporal segments, end uses, stages of production, and quality tiers. Likewise, 'transport cost' means any cost of moving product between segments. Set a ceiling at the "summer price" and you eliminate the incentive to 'transport' oil to winter via storage. Cap refined-product prices and minute differences in refining costs can redirect nearly all crude toward gasoline, starving diesel and jet fuel. Segments are manifold but the mechanism is the same: price controls induce seller indifference across allocations so any friction, however small, selects a corner; and small shifts in friction flip the system between corners.

Formally, a binding ceiling  $\bar{p}$  fixes the aggregate quantity at  $\bar{Q} = S(\bar{p})$ , where  $S$  is the aggregate supply curve. Let  $D$  denote aggregate demand. We assume that  $\bar{p}$  is binding in the sense that  $D(\bar{p}) > S(\bar{p})$ . There are  $n \geq 1$  segmented sub-markets. In market  $i$ , inverse demand  $P_i(\cdot)$  is continuous and nonincreasing on  $[0, D_i(\bar{p})]$ .

We formalize market segmentation through the concept of a decomposition: a partition of aggregate demand into submarket demands. A decomposition specifies how many consumers in each submarket are willing to buy at any given price. The inverse demand  $P_i(q_i)$  in submarket  $i$ , the price at which exactly  $q_i$  units would be demanded, represents the marginal willingness to pay, or *shadow price*, when quantity  $q_i$  is allocated to that market.

**Definition 1.** A collection of direct demand functions  $\{D_i\}_{i=1}^n$  with  $D_i$  continuous and nonincreasing in price is a *decomposition* if  $D(p) = \sum_i D_i(p)$  on  $[0, \infty)$ .

The price ceiling  $\bar{p}$  constrains feasible allocations in two ways. First, total quantity cannot exceed supply:  $\sum_i q_i = \bar{Q} \equiv S(\bar{p})$ . Second, no submarket can receive more than its demand at the ceiling price, or the local price would fall below the ceiling. Define

$\bar{q}_i \equiv D_i(\bar{p})$  as the maximum quantity submarket  $i$  can absorb at price  $\bar{p}$ . The feasible set is then:

$$\mathcal{F} := \left\{ q \in \mathbb{R}_+^n : 0 \leq q_i \leq \bar{q}_i \forall i, \sum_{i=1}^n q_i = \bar{Q} \right\}.$$

This is a convex polytope (Grünbaum 2003), meaning the intersection of a hyperplane (the adding-up constraint) with a box (the upper and lower bounds). Its extreme points, or vertices, correspond to allocations where all but one submarket is either completely served ( $q_i = \bar{q}_i$ ) or completely starved ( $q_i = 0$ ).

To measure welfare, we focus on consumer surplus. In submarket  $i$ , consumer surplus at allocation  $q_i$ , measured relative to the ceiling price  $\bar{p}$ , is the integral of willingness to pay above the price paid:

$$W_i(q_i) := \int_0^{q_i} [P_i(x) - \bar{p}] dx.$$

Aggregating across submarkets gives total consumer surplus:  $W(q) := \sum_{i=1}^n W_i(q_i)$ .

It will sometimes be convenient to work with *gross* surplus, or the area under the inverse demand curve without subtracting the price paid:

$$\tilde{W}_i(q_i) := \int_0^{q_i} P_i(x) dx, \quad \tilde{W}(q) := \sum_{i=1}^n \tilde{W}_i(q_i).$$

Since  $W(q) = \tilde{W}(q) - \bar{p} \bar{Q}$  and total quantity  $\bar{Q}$  is fixed on  $\mathcal{F}$ , maximizing consumer surplus  $W$  is equivalent to maximizing gross surplus  $\tilde{W}$ . This equivalence simplifies the analysis: we can ignore the constant  $\bar{p} \bar{Q}$  term and focus on gross surplus alone.

What allocation maximizes consumer surplus? Under standard conditions, surplus is maximized when the marginal value of the good is equalized across all submarkets that receive positive supply. If one market has a higher shadow price than another, we could increase total surplus by reallocating a unit from the low-value market to the high-value one. This intuition guides the following definition.

**Definition 2.** An allocation  $q \in \mathcal{F}$  *equalizes shadow prices* if there exists  $p^* \geq \bar{p}$  such that for every  $i$ ,

- I.  $0 < q_i < \bar{q}_i \implies P_i(q_i) = p^*$ ,
- II.  $q_i = \bar{q}_i \implies P_i(q_i) \geq p^*$ , and
- III. if  $q_i = 0$ , then  $P_i(0) \leq p^*$ .

**Proposition 1.**  $q^*$  maximizes  $W$  over  $\mathcal{F}$  if and only if  $q^*$  equalizes shadow prices.

The proof is standard.

Letting  $q^* \in \mathcal{F}$  denote an equal-shadow-price allocation from Proposition 1, we now note the following decomposition.

**Definition 3.** Let  $q^* \in \mathcal{F}$  denote an equal-shadow-price allocation from Proposition 1. The *misallocation deadweight loss* of a feasible allocation  $q \in \mathcal{F}$  is the welfare shortfall relative to  $q^*$ :

$$\mathcal{L}_{Mis}(q) := W(q^*) - W(q) = \sum_{i=1}^n [W_i(q_i^*) - W_i(q_i)].$$

This definition isolates the welfare loss from *how* the fixed total  $\bar{Q}$  is distributed across submarkets. It holds constant the aggregate quantity reduction (the source of the Harberger triangle) and asks: given that we must allocate exactly  $\bar{Q}$  units, how much additional surplus is destroyed by allocating them inefficiently?

To build intuition, consider the expression in integral form:

$$\mathcal{L}_{Mis}(q) = \sum_{i=1}^n \int_{q_i}^{q_i^*} [P_i(x) - \bar{p}] dx = \sum_{i=1}^n \int_{q_i}^{q_i^*} P_i(x) dx,$$

where the second equality uses  $\sum_i (q_i^* - q_i) = 0$  to cancel the  $\bar{p}$  terms. Each integral measures the value of the units that submarket  $i$  receives under the efficient allocation but not under  $q$  (if  $q_i < q_i^*$ ), or the value of excess units that  $i$  receives under  $q$  but not

under the efficient allocation (if  $q_i > q_i^*$ ). Markets that are under-served lose high-value units; markets that are over-served gain low-value units. The difference is pure waste.

The misallocation deadweight loss has an important economic interpretation: it represents the value that would be created if arbitrageurs could freely reallocate the fixed supply  $\bar{Q}$  across markets. Under normal market conditions, price differences incentivize such reallocation. But when prices are frozen at  $\bar{p}$ , these incentives vanish. The welfare loss is precisely the forgone gains from trade. They are the dollars left on the table when goods do not flow to their highest-value uses.

## 4.1 Worst-Case Allocations

We have established that equalizing shadow prices across submarkets minimizes deadweight loss for any fixed aggregate quantity  $\bar{Q}$ . We now characterize the opposite extreme: which allocation *maximizes* deadweight loss?

Recall that

$$V(q) \equiv \mathcal{L}_{Mis}(q) = \underbrace{\sum_i \int_0^{q_i^*} P_i(x) dx}_{\text{constant in } q} - \sum_i \int_0^{q_i} P_i(x) dx = W(q^*) - W(q).$$

As we noted earlier, maximizing misallocation  $V(q)$  is equivalent to minimizing the gross consumer surplus  $\tilde{W}(q) := \sum_i \int_0^{q_i} P_i(x) dx$  over the feasible set  $\mathcal{F}$ .

Intuitively, the worst case concentrates supply in markets where it generates the least value. Markets with high choke prices receive nothing; markets with low shadow prices are flooded.

**Theorem 1.** Assume each  $P_i$  is continuous and weakly decreasing on  $[0, \bar{q}_i]$  and  $\mathcal{F} \neq \emptyset$ . Then,

- (i)  $V$  is maximized at an extreme point of  $\mathcal{F}$ , where  $q_i \in \{0, \bar{q}_i\}$  for all but at most one  $i$ .

(ii) For any worst-case allocation  $q^w \in \mathcal{F}$ , there exists a cutoff  $\lambda_{\text{worst}} \in [0, \infty)$  such that for every market  $i$ ,

$$\begin{aligned} \text{if } 0 < q_i^w < \bar{q}_i, & \quad \text{then } P_i(q_i^w) = \lambda_{\text{worst}}, \\ \text{if } q_i^w = 0, & \quad \text{then } P_i(0) \geq \lambda_{\text{worst}}, \\ \text{if } q_i^w = \bar{q}_i, & \quad \text{then } P_i(\bar{q}_i) \leq \lambda_{\text{worst}}. \end{aligned}$$

(iii) If  $\bar{Q} \leq \bar{q}_j$  for some  $j$ , then among single-market vertices  $(\bar{Q}, 0, \dots, 0)$  the worst case is any

$$j \in \arg \min_i \int_0^{\bar{Q}} P_i(x) dx,$$

that is, the market with the smallest average value up to  $\bar{Q}$  (not necessarily the smallest marginal price  $P_i(\bar{Q})$ ).

We defer the formal proof of this theorem to Appendix A.1. Part (ii) provides necessary KKT-type conditions for any worst-case allocation; identifying the global worst among candidate vertices requires comparing average values as in part (iii). Overall, the worst outcome is form of all-or-nothing. Markets with choke prices above the threshold receive nothing; those below it receive everything. This corner structure maximizes the shadow price gap, hence the welfare loss.

## 5 The Chaos of Price Controls

The previous section characterized the range of possible welfare outcomes: from the best case (equalizing shadow prices) to the worst case (concentrating supply in low-value markets). But this leaves open a crucial question: *which* allocation should we expect to observe in practice?

Under market clearing, arbitrage answers this question. Under price controls, there is

no arbitrage. Instead, allocation depends on parameters that would otherwise be irrelevant, and the dependence is discontinuous.

Formally, we show small perturbations in underlying parameters can cause discontinuous jumps in allocations and welfare under price controls. The key insight is that once price variation is removed, the equilibrium allocation becomes determined by arbitrarily small differences in costs or capacities.

## 5.1 Setup

Let  $\theta \in \Theta \subset \mathbb{R}^m$  be a compact parameter space governing sub-market inverse demands  $P_i(x; \theta)$ , unit costs  $c_i(\theta)$ , and total quantity  $\bar{Q}(\theta) > 0$ . We assume (i) *Demand regularity*: for each  $i$  and every  $\theta$ , the map  $x \mapsto P_i(x; \theta)$  is continuous and strictly decreasing; (ii) *Parameter continuity*: for each  $x$ , the map  $\theta \mapsto P_i(x; \theta)$  is continuous. We also assume (iii) *Cost continuity*: sub-market unit costs  $c_i(\theta)$  and the total quantity  $\bar{Q}(\theta) > 0$  are continuous in  $\theta$ .

Without price controls, the unique welfare-maximizing allocation  $q^*(\theta)$  varies continuously with  $\theta$  by Berge's Maximum Theorem. Small changes in parameters produce small changes in allocations and welfare.

## 5.2 Discontinuity Under Price Controls

Now impose a binding ceiling  $\bar{p}$ . Define  $\bar{q}_i(\theta) := D_i(\bar{p}; \theta)$  and  $\bar{Q}(\theta) := S(\bar{p}; \theta)$ . Under price controls, profit-maximizing suppliers minimize delivery costs since all units sell at the same price  $\bar{p}$ . Thus, the allocation is determined by cost minimization:

$$\min_{q \in \mathcal{F}(\theta)} c(\theta) \cdot q,$$

where  $\mathcal{F}(\theta) = \{q \in \mathbb{R}_+^n : \sum_{i=1}^n q_i = \bar{Q}(\theta), 0 \leq q_i \leq \bar{q}_i(\theta)\}$ .

Under generic conditions (distinct costs across markets, and total quantity not exactly equal to any subset sum of capacities), the optimizer has a stark structure: markets are filled in order of increasing cost, with at most one market partially filled. Crucially, when two markets have nearly equal costs, an infinitesimal parameter change can flip the entire allocation between them.

### 5.3 Chaos Result

Let two feasible allocations  $v$  and  $w$  differ only in which markets receive supply— $v$  fills certain low-cost markets while  $w$  fills others. Specifically, suppose allocation  $w$  gives market  $s$  more units than  $v$  does ( $w_s > v_s$ ), while market  $r$  receives fewer units ( $w_r < v_r$ ), with the same total quantity. Define the welfare jump—which, here, equals the difference in gross surplus—between them as

$$\Delta W = \int_{v_s}^{w_s} P_s(x)dx - \int_{w_r}^{v_r} P_r(x)dx,$$

where  $r$  and  $s$  are the markets whose allocations differ.

**Theorem 2** (Chaos). *Suppose costs  $c_i(\theta)$  are such that two adjacent vertex allocations (vertices of  $\mathcal{F}$  differing in exactly two coordinates)  $v$  and  $w$  are both optimal at some parameter  $\theta^*$ . If  $\Delta W \neq 0$  (a generic condition), then for every neighborhood  $U$  of  $\theta^*$  there exist smooth parameter paths through  $U$  along which*

- (i) *The optimal allocation jumps discontinuously between  $v$  and  $w$ ;*
- (ii) *Welfare jumps by  $+|\Delta W|$  along one path and  $-|\Delta W|$  along another.*

*In particular, welfare is not locally monotone in parameters: arbitrarily small perturbations can move welfare up or down by discrete amounts.*

**Corollary 1.** *For every neighborhood  $U$  of  $\theta^*$ , there exist parameters  $\theta^-, \theta^+ \in U$  with  $\|q^*(\theta^+) - q^*(\theta^-)\|_1 = 2\Delta > 0$ , where  $\Delta$  is the quantity shifted between markets.*

The proofs, which formalize the geometry of normal cones and construct explicit crossing paths, appear in Appendix [A.2](#).

This result explains the patchwork pattern of Figure 1. Under price controls, which markets receive supply depends on cost parameters that may shift unpredictably with weather, refinery maintenance, or regulatory discretion. A small change—say, a pipeline repair that marginally reduces delivery costs to New Jersey—can discontinuously redirect supply away from New York, even though both states’ underlying demands are nearly identical.<sup>2</sup>

The theorem also explains why which markets are starved is often volatile over time. Week-to-week fluctuations in transportation costs, inventory positions, or bureaucratic priorities could flip allocations between equilibria, generating the erratic patterns documented in contemporary reports.

More broadly, the result shows that price controls introduce a fundamental unpredictability into markets. When prices cannot signal value, allocations become hypersensitive to “nuisance parameters” that would be irrelevant under market clearing. This hypersensitivity—chaos in the mathematical sense—is not a market failure but a direct consequence of suppressing the price mechanism. Ironically, the chaos of price controls often fuels demands for even tighter controls and increasingly politicized and bureaucratized allocations.

2. The Chaos Theorem assumes agents are rational cost-minimizers which pushes allocations to corner solutions. In practice, long-term contracts, sticky relationships, or regulatory inertia may prevent immediate jumps to vertices. However, over time, competitive pressures tend to push allocations toward these extreme points, making the chaos result increasingly relevant as the control regime persists. In this sense, the Chaos Theorem is a worst-case outcome.

## 5.4 Simulation

We illustrate the Chaos Theorem with simulations of 100 gasoline markets arranged on a  $10 \times 10$  grid. Each city has a per-unit delivery cost drawn uniformly from  $[0, 0.1]$ . We use a demand specification with a finite choke price, so welfare is well-defined even when markets receive zero.<sup>3</sup> Aggregate supply is fixed at  $Q = 150$  units, and we impose a price control at 80% of the market-clearing price.

Under price controls, the allocation follows a greedy rule: fill the lowest-cost city to capacity, then the next-lowest, until supply is exhausted. This produces a vertex allocation where served cities receive their full demand while roughly 30 cities receive nothing.

Figure 4 shows allocations under three random cost draws. The top row shows free-market allocations; the bottom row shows price-control allocations for the same costs. Three patterns emerge. First, free-market allocations are nearly identical across scenarios—small cost differences produce small allocation differences. Second, under price controls, many markets receive zero (yellow). Third, under price controls, different cost draws produce radically different allocations. This is the Chaos Theorem: small changes in nuisance parameters dramatically change the final allocation. Misallocation in these scenarios generates a welfare loss of roughly 13%.

Cost structures may also have systematic components: locations close to refineries may have lower costs. These produce different spatial patterns but the same corner-solution logic.

3. We use a Hill (sigmoidal) demand function; see Appendix C for details.

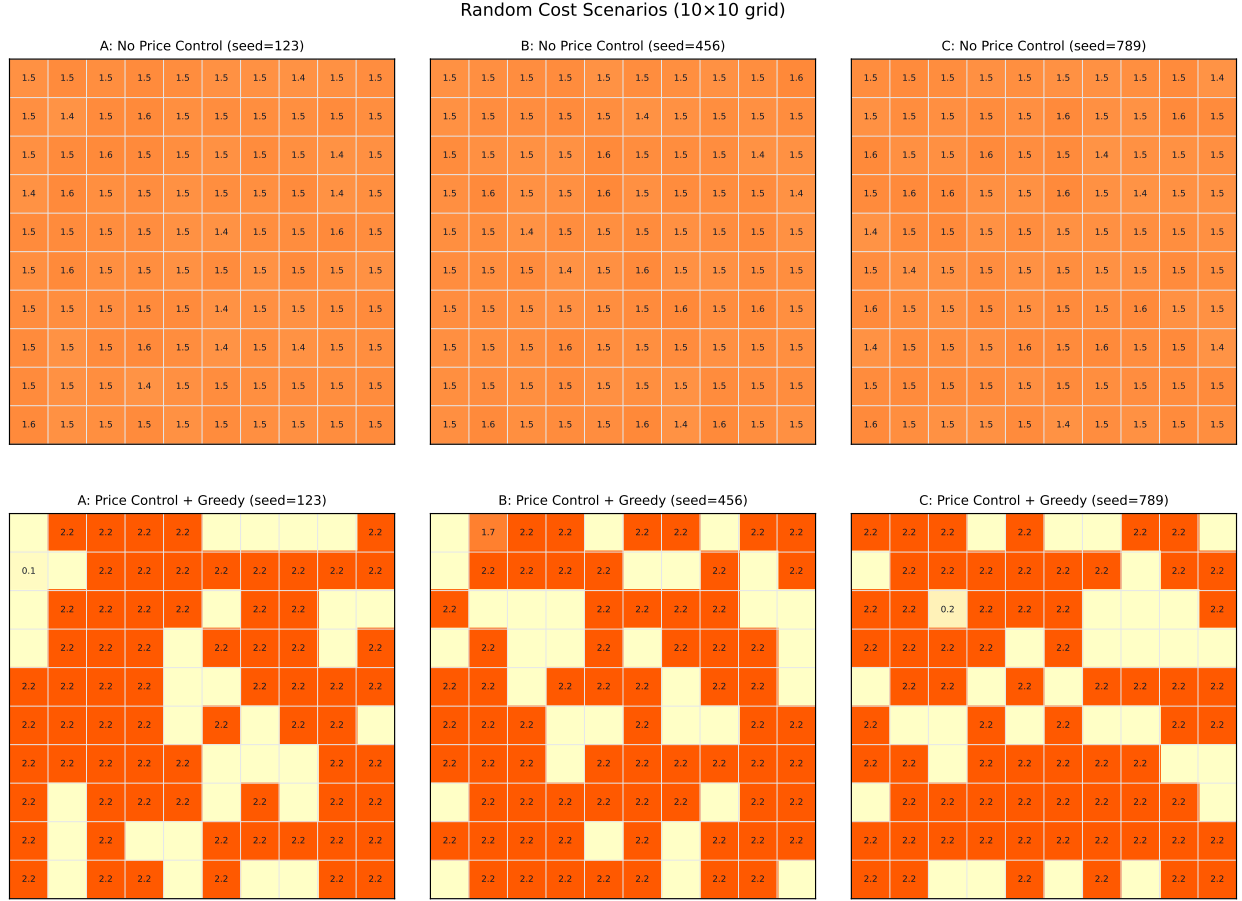


Figure 4: Allocation of a fixed supply ( $\bar{Q} = 150$ ) across 100 cities under free markets (top) versus price controls (bottom). Each column is a different random draw of delivery costs. Under free markets, quantities vary smoothly. Under price controls, low-cost cities fill to capacity while approximately 30 cities go unserved.

## 6 Robust Bounds on Misallocation

The Chaos Theorem tells us that under price controls we should expect corner allocations, far from market equilibria. We know, rationed stations received only 68% of baseline quantity and often no quantity at all. Elasticity estimates identify demand locally near equilibrium, not at these depressed allocations. Rather than extrapolating via functional form assumption, we develop a partial identification approach. Given only the observed allocation, the ceiling price, bounds on local demand elasticities, and an anchored point

on each demand curve (or a bounded interval for that anchor), we derive sharp bounds on misallocation. This is not sensitivity analysis within a parametric family. We do not commit to any functional form. Instead, we ask: across all inverse demand functions consistent with slope bounds, what are the largest and smallest possible welfare losses? The output is an identified interval, not a point estimate, and the interval covers welfare under all robustly possible allocations.

In market  $i$ , the unknown inverse demand  $P_i: [0, q_i^{\max}] \rightarrow \mathbb{R}_+$  is continuous and nonincreasing in quantity  $q$ , where each bound  $q_i^{\max} \in (0, \infty)$  is an exogenous upper bound on feasible quantities (representing physical capacity, infrastructure limits, or maximum historical consumption), distinct from the demand-derived  $\bar{q}_i = D_i(\bar{p})$  used elsewhere. A binding ceiling  $\bar{p} > 0$  is imposed. We observe the delivered allocation  $q^{\text{obs}} = (q_1^{\text{obs}}, \dots, q_n^{\text{obs}})$ , where

$$\bar{Q} := \sum_{i=1}^n q_i^{\text{obs}} \in \left[0, \sum_i q_i^{\max}\right]$$

.

**Assumption 1.** For all  $i$ ,  $P_i$  is nonincreasing and satisfies

- I.  $P_i(q_i^{\text{obs}}) = p_{0,i} = \bar{p} - b_i$  with  $b_i \in [\underline{b}_i, \bar{b}_i]$ .
- II. There exist  $g_{i,L} < g_{i,U} \leq 0$  with  $g_{i,L} \leq P'_i(q) \leq g_{i,U}$  for a.e.  $q \in [0, q_i^{\max}]$ .
- III.  $P_i(0) \leq M_i < \infty$
- IV.  $P_i \in W^{1,\infty}([0, q_i^{\max}])$ , the space of bounded Lipschitz-continuous functions on  $[0, q_i^{\max}]$ .

The first three assumptions are the economically meaningful ones. Allowing  $g_{i,U} = 0$  admits locally flat demand segments; the strict inequality  $g_{i,L} < g_{i,U}$  ensures the slope bounds are distinct. The last one is technical, guaranteeing that the various objects we

construct are well-defined. Let  $\mathcal{P}_i$  be the set of  $P_i$  satisfying Assumption 1 and  $\mathcal{P} := \times_{i=1}^n \mathcal{P}_i$ . We assume  $\mathcal{P} \neq \emptyset$ .

By Part II. of Assumption 1 and the fundamental theorem of calculus,  $P_i(q_i) = p_{0,i} + \int_{q_i^{\text{obs}}}^{q_i} P'_i(s) ds$  lies between the two affine functions  $p_{0,i} + g_{i,L}(q_i - q_i^{\text{obs}})$  and  $p_{0,i} + g_{i,U}(q_i - q_i^{\text{obs}})$ . We solve these bounds for  $q_i$  at a price  $p$ . On  $[0, \bar{q}_i]$ , for fixed  $p$ , we denote

$$\ell_i(p) := \max \left\{ 0, \min \left\{ q_i^{\text{obs}} + \frac{p - p_{0,i}}{g_{i,U}}, q_i^{\text{obs}} + \frac{p - p_{0,i}}{g_{i,L}} \right\} \right\}, \quad \text{and}$$

$$u_i(p) := \min \left\{ q_i^{\text{max}}, \max \left\{ q_i^{\text{obs}} + \frac{p - p_{0,i}}{g_{i,U}}, q_i^{\text{obs}} + \frac{p - p_{0,i}}{g_{i,L}} \right\} \right\}.$$

Then, writing the left-continuous generalized inverse

$$q_i(p) := \inf \{x \in [0, q_i^{\text{max}}] : P_i(x) \leq p\}$$

with the convention that  $q_i(p) = q_i^{\text{max}}$  when this set is empty (i.e., when  $p < P_i(q_i^{\text{max}})$ ), it must be that  $q_i(p) \in [\ell_i(p), u_i(p)]$  for all  $p$ . Define  $L(p) := \sum_i \ell_i(p)$ ,  $U(p) := \sum_i u_i(p)$ , and

$$\mathcal{I} := \{p \in \mathbb{R} : L(p) \leq \bar{Q} \leq U(p)\}.$$

At the price level  $p$ ,  $\ell_i(p)$  and  $u_i(p)$  are the smallest and largest (respectively) quantities in market  $i$  that are consistent with (i) passing through  $(q_i^{\text{obs}}, p_{0,i})$  and (ii) obeying the slope bounds. The set  $\mathcal{I}$  is then the set of candidate shadow prices  $p$  for which the economy can possibly have total quantity  $\bar{Q}$ . That is, at such a  $p$ , the interval constraints across markets are compatible with  $\sum_i q_i(p) = \bar{Q}$ .

For  $P \in \mathcal{P}$ , we measure misallocation relative to the equal-shadow split:

$$\Phi(P) := \sum_{i=1}^n \int_{q_i^{\text{obs}}}^{q_i^*(P)} (P_i(x) - p^*(P)) dx,$$

where  $p^*(P)$  is the multiplier on  $\sum_i q_i = \bar{Q}$ .<sup>4</sup> Note that using  $p^*$  instead of  $\bar{p}$  is harmless since  $\sum_i (q_i^* - q_i^{\text{obs}}) = 0$ . Denote  $\bar{\Phi} := \max_{P \in \mathcal{P}} \Phi(P)$  and  $\underline{\Phi} := \min_{P \in \mathcal{P}} \Phi(P)$ . Then, Note that using  $p^*$  instead of  $\bar{p}$  is harmless since  $\sum_i (q_i^* - q_i^{\text{obs}}) = 0$ . Denote  $\bar{\Phi} := \max_{P \in \mathcal{P}} \Phi(P)$  and  $\underline{\Phi} := \min_{P \in \mathcal{P}} \Phi(P)$ . Then,

**Lemma 1.** *We have*

$$\bar{\Phi} = \max_{p \in \mathcal{I}} \left\{ \bar{Q}p - \sum_i q_i^{\text{obs}} p_{0,i} - \sum_{i: p \geq p_{0,i}} \int_{p_{0,i}}^p \ell_i(s) \, ds + \sum_{i: p < p_{0,i}} \int_p^{p_{0,i}} u_i(s) \, ds \right\}, \quad (1)$$

and

$$\underline{\Phi} = \min_{p \in \mathcal{I}} \left\{ \bar{Q}p - \sum_i q_i^{\text{obs}} p_{0,i} - \sum_{i: p \geq p_{0,i}} \int_{p_{0,i}}^p u_i(s) \, ds + \sum_{i: p < p_{0,i}} \int_p^{p_{0,i}} \ell_i(s) \, ds \right\}. \quad (2)$$

That is, each inner optimizer satisfies  $q_i(s) \in \{\ell_i(s), u_i(s)\}$  for almost every  $s \neq p$ , and at  $s = p$  (if needed) at most one  $q_i(p) \in (\ell_i(p), u_i(p))$  in order to satisfy  $\sum_i q_i(p) = \bar{Q}$ .

The proof appears in Appendix A.3.

Lemma 1 is the heart of this robust bounds approach. It turns the bound-finding problem over the huge class  $\mathcal{P}$  into a one-dimensional program over  $p \in \mathcal{I}$ ; and, moreover, argues that the optimizer saturates the endpoints. The key simplification is that for any candidate common shadow price  $p$ , the unknown objects enter only through the inverse-quantity functions  $q_i(\cdot)$ , and the objective is *linear* in those functions. Thus, conditional on  $p$ , the worst or best case pushes  $q_i(\cdot)$  to its pointwise extremes  $\ell_i(\cdot)$  or  $u_i(\cdot)$  almost everywhere, and the remaining optimization is only over the scalar  $p$ .

**Theorem 3.** *Both  $\bar{\Phi}$  and  $\underline{\Phi}$  are attained by some  $P^* \in \mathcal{P}$ . Moreover, each  $P_i^*$  may be chosen piecewise affine with a.e. derivative  $P_i^{*'}(q) \in \{g_{i,L}, g_{i,U}\}$  on  $[0, q_i^{\max}]$ .*

4. Under a specific demand function,  $\Phi$  equals the misallocation loss  $\mathcal{L}_{\text{Mis}}$  from Section 7. Here we optimize over all admissible  $P$ .

The proof appears in Appendix [A.4](#).

**Corollary 2.** *Suppose we also optimize over  $p_{0,i} \in [\bar{p} - \bar{b}_i, \bar{p} - \underline{b}_i]$ . If the candidate shadow price is at least as large as the price implied by the observed quantity in market  $i$ ; viz.,  $p \geq P_i(q_i^{\text{obs}})$  and none of the upper or lower bounds on quantities bind over the relevant price range, the upper bound is produced by the largest bias and the lower bound by the smallest bias.*

Theorem 3 establishes that the bounds  $[\underline{\Phi}, \overline{\Phi}]$  are *sharp*: they are attained by demand functions in the permitted class. This sharpness distinguishes partial identification from sensitivity analysis. Sensitivity analysis with linear demand would vary the slope  $b$  and report how misallocation changes, yielding the same numerical interval when the choke-price constraint is non-binding. With a binding  $P(0) \leq M$ , the robust bounds can differ because the extremal piecewise-affine demands can kink to satisfy the choke while steeper linear extrapolations cannot. But sensitivity analysis cannot rule out the possibility that some nonlinear demand (convex, concave, or oscillating within the slope bounds) produces misallocation outside that interval.

The theorem closes this gap. By the fundamental theorem of calculus, any demand function with  $P'(q) \in [g_L, g_U]$  must lie within a cone emanating from the observed point. Since misallocation is an integral of the demand curve, it inherits these bounds. The theorem confirms that the extreme misallocation is achieved at the boundary of this cone, by piecewise affine demand with slopes in  $\{g_L, g_U\}$ , not by some exotic function in the interior. The bounds from linear demand are therefore not conservative approximations; they are exact over the infinite-dimensional class of all Lipschitz functions satisfying the slope constraints.

## 7 Illustrating Chaos: The 1973–74 Gasoline Crisis

In August of 1971, President Nixon froze all wages and prices in the United States. Many prices were unfrozen after the 90-day scheduled period, but petroleum remained subject to controls with various modifications until August of 1973 when Special Rule No. 1 established mandatory controls for petroleum specifically <sup>5</sup>.

Price controls on oil and the sporadic shortages were thus already in place well before the Oil Embargo began in October of 1973. The embargo, however, dramatically increased the market price of oil above the controlled price, transforming what had been moderate distortions into severe shortages. From October of 1973 to January of 1974 the price of oil tripled. Over the first shock, quantity consumed fell by about 9% relative to trend (Yergin 1991).

Quickly following the embargo, the Emergency Petroleum Allocation Act of 1973 (EPAA) ratified President Nixon's earlier executive orders with legislated price controls and an allocation system based pro-rata on 1972 levels. If total supply fell to 90% of 1972's volume, for example, each buyer would receive 90% of their 1972 allocation. This basic system was then adjusted with numerous exceptions, prioritizing industries such as national defense, essential services, agriculture, and independent refiners, all under an overarching "fair and equitable" guideline (Bradley 1997).

We begin with a formal analysis of the most visible portion of the petroleum allocation under price controls. Namely, the allocation of gasoline across geographies. We then turn to an informal discussion of misallocation across time, sector and other segmentations.

5. See Bradley 1997 for a definitive account of the crisis.

## 7.1 AAA Data

We digitize station-level survey data collected by the AAA during February 1974. Figure 1 displays the cross-sectional variation in rationing (out-of-fuel closures + purchase limits). The mean out-of-fuel rate by state was 8.2%, but this average masks striking heterogeneity. The survey reports that 10.1% of stations were closed (out of fuel), 27.8% were limiting purchases, and 62.1% were operating normally. We combine this station-level classification with 1972 gasoline station counts from the U.S. Census of Retail Trade. Our sample includes all states except Alabama and Alaska, which lacked AAA survey coverage.

## 7.2 Welfare Measures

The Harberger deadweight loss measures the welfare cost of the aggregate quantity reduction, assuming the reduced supply is allocated efficiently:

$$\mathcal{L}_{Harb} = \tilde{W}(q^{base}) - \tilde{W}(q^*) - \bar{p} \cdot (Q^{base} - \bar{Q}) \quad (1)$$

Here  $\tilde{W}(q) := \sum_i \int_0^{q_i} P_i(x) dx$  denotes gross surplus (the area under demand), in contrast to the net surplus  $W$  defined earlier. The final term subtracts avoided expenditure at the controlled price: consumers who cannot buy the reduced quantity also do not pay  $\bar{p}$  for it. The misallocation loss  $\mathcal{L}_{Mis} = W(q^*) - W(q^{obs})$  captures the additional welfare destruction from inefficient distribution of the reduced supply, as defined in Section 3.

We express these welfare losses as percentages of *baseline expenditure*: total consumer spending before the crisis,  $p^{base} \times Q^{base}$ . With our normalization ( $p^{base} = 1$ ,  $Q^{base} = 1$ ), baseline expenditure equals unity. This metric provides economic interpretation: a misallocation loss of 3.6% means consumers lost welfare equivalent to 3.6% of their pre-crisis gasoline spending.

Our key statistic is the *Misallocation Ratio*:

$$\mathcal{R} = \frac{\mathcal{L}_{Mis}}{\mathcal{L}_{Harb}} \quad (2)$$

A ratio  $\mathcal{R} = 1$  means misallocation doubles the welfare cost relative to a standard Harberger analysis;  $\mathcal{R} > 1$  means misallocation is the dominant source of loss. With efficient rationing,  $\mathcal{R} = 0$ .

### 7.3 Allocation

We aggregate stations into two markets: open (62%) and closed/limiting (38%). “Out of fuel” is a point-in-time status from the AAA survey, not a period-average of  $q = 0$ . Our two-market calibration aggregates closed/limiting stations into a single partially-served submarket. The key economic mechanism is that the controlled price  $\bar{p}$  lies below the market-clearing price. At  $\bar{p}$ , quantity demanded exceeds quantity supplied. Open stations satisfy their customers; closed and limiting stations cannot.

Under a vertex allocation, open stations consume their full demand at the controlled price while closed stations receive the residual. We assume  $\bar{p} = 0.8$ , consistent with (Frech and Lee 1987). With elasticity bounds  $\varepsilon \in [0.2, 0.4]$ , baseline-anchored linear demand implies

$$q_O \in [1.04, 1.08].$$

Closed/limiting stations receive the residual

$$q_C = \frac{\bar{Q} - (1 - s) \cdot q_O}{s} \Rightarrow q_C \in [0.63, 0.70].$$

For the baseline calibration, we use  $\varepsilon = 0.3$ , which gives  $q_O = 1.06$  and  $q_C \approx 0.67$ . This allocation satisfies the aggregate constraint and exhibits exactly the corner-solution

structure predicted by the Chaos Theorem.

## 7.4 Station-Level Robust Bounds

Two features of our setting make partial identification essential. First, extreme allocations are where functional form does most of the work. Our welfare calculations integrate inverse demand over quantity ranges extending to  $q \approx 0.67$  for closed/limiting stations. Elasticity estimates come from observed price-quantity variation around market equilibrium, identifying the slope of demand locally near  $q = 1$ , not at  $q = 0.68$ . To compute welfare at these allocations, we must extrapolate beyond where demand is identified. Linear extrapolation from an elasticity of 0.2 implies  $P(0) = 6$ ; from 0.4, it implies  $P(0) = 3.5$ . CES demand diverges entirely as  $q \rightarrow 0$ , requiring an arbitrary choke-price normalization. The welfare difference between these extrapolations determines whether misallocation losses are 4% or 16% of baseline expenditure.

Second, unequal allocations are the generic prediction. The Chaos Theorem tells us to expect extreme dispersion, and the February 1974 data deliver exactly that: 10% of stations closed and 28% limiting purchases while 62% operated normally. This is not a smooth 9% quantity reduction spread uniformly across stations. At the controlled price, open stations satisfy their customers at  $q = 1.06$  while closed/limiting stations sell out or ration at  $q = 0.67$ . This gap is exactly the configuration where parametric welfare calculations are most fragile.

Taken together, the theory predicts allocation dispersion, the data show dispersion, and dispersion is where functional form assumptions bite hardest. We do not want our welfare estimates hostage to how we extrapolate demand into regions no estimation has ever reached. The robust bounds approach sidesteps this problem. We impose only local, transparent restrictions (slope bounds from elasticity estimates and a finite choke price) and optimize over all inverse demands consistent with these assumptions.

We apply this framework to the station-level data. The AAA survey reports the *share* of stations limiting purchases or out of fuel, not gallons sold. Mapping status shares into quantities requires one additional input: the quantity  $q_{open}$  that open stations sell at the controlled price. Any downward-sloping demand anchored at baseline implies  $q_{open} > 1$  when  $\bar{p} < p^{base}$ , because lower prices raise quantity demanded. With elasticity bounds  $\varepsilon \in [0.2, 0.4]$  and  $\bar{p} = 0.8$ , linear demand gives  $q_{open} \in [1.04, 1.08]$ . For the baseline calibration used in figures and in the state mapping step, we set  $q_{open} = 1.06$ . Given  $q_{open}$ , the quantity  $q_{non-open}$  follows from requiring that the station-weighted national average equals aggregate supply  $\bar{Q} = 0.91$ ; this yields  $q_{non-open} \approx 0.67$ . This calibration step is the only place where functional form enters. The robust welfare results below are reported as intervals.

At the controlled price  $\bar{p} = 0.8$ , open stations (62%) satisfy demand at  $q_O \in [1.04, 1.08]$  while closed/limiting stations (38%) receive the residual  $q_C \in [0.63, 0.70]$ . We use the baseline calibration  $q_O = 1.06$  and  $q_C = 0.67$  for the plotted benchmark. For elasticity bounds  $\varepsilon \in [0.2, 0.4]$ , the slope bounds are  $g \in [-5, -2.5]$ .<sup>6</sup>

Three figures illustrate how these slope bounds translate into welfare uncertainty using the baseline calibration ( $q_O = 1.06$ ,  $q_C = 0.67$ ). Figure 5 shows the demand curves consistent with the slope bounds and observed allocation when no choke constraint is imposed. Solid segments are pinned down by the data and slope restrictions; dashed segments are admissible extensions. These no-choke bounds are our headline station-level intervals.

Figure 6 adds a choke constraint  $P(0) \leq M = 4$ . The key intuition is geometric. In the lower-loss panel, the steep branch would extrapolate to  $P(0) = 6 > 4$ , so the admissible

6. Throughout, “steep” and “flat” refer to the inverse demand curve  $P(Q)$ . A steep inverse demand (large  $|g|$ , low elasticity) means price falls rapidly as quantity rises. This corresponds to a *flat* demand curve  $Q(P)$ , where quantity responds little to price changes. The figures plot  $P$  against  $Q$ , so visual steepness matches  $|g|$ .

Station-Level Demand Curves Consistent with Observed Rationing (No Choke) (displayed in per-station units)

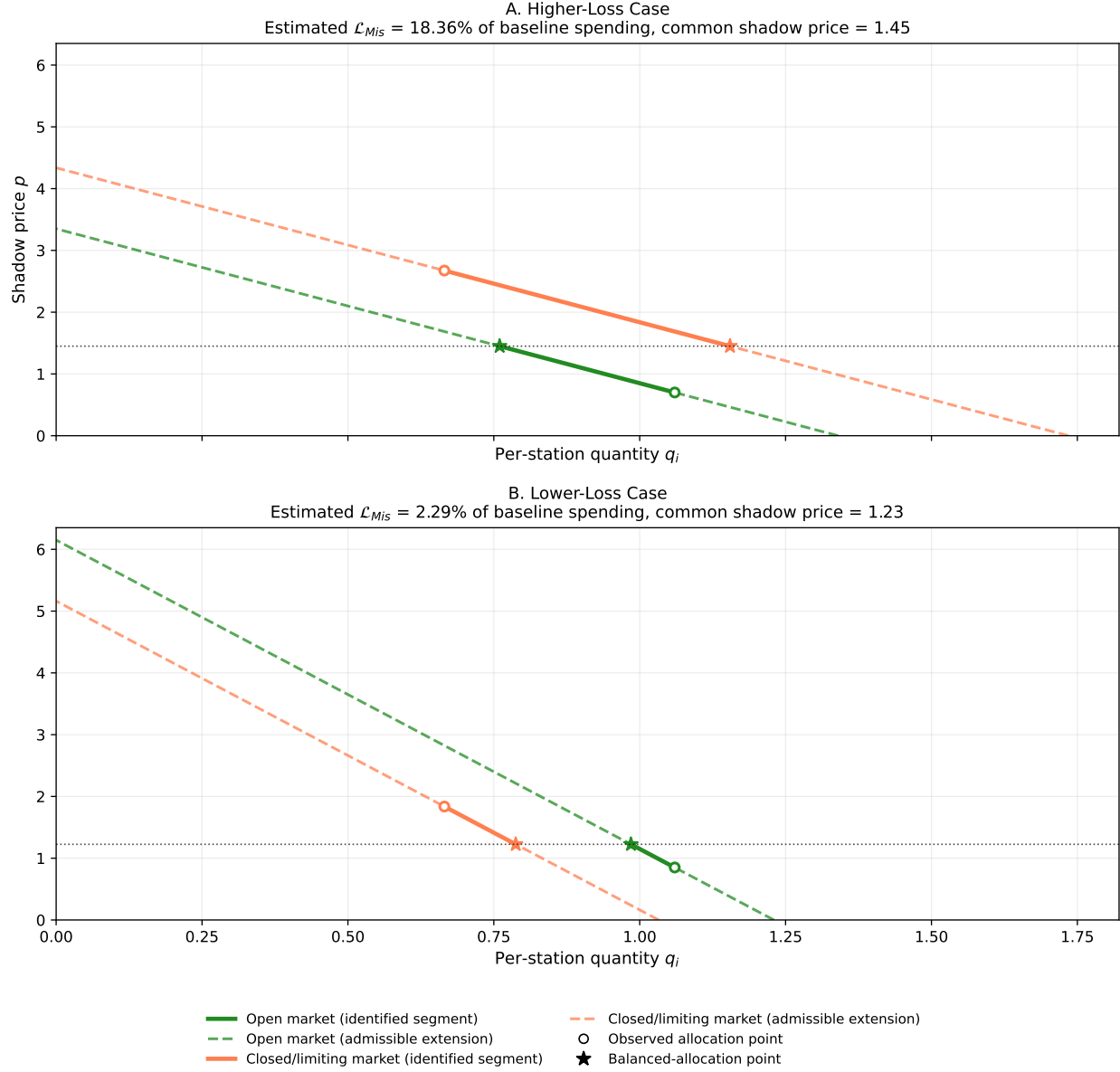


**Figure 5: Station-Level Demand Curves Without Choke.** The two panels show high-loss and low-loss demand configurations consistent with observed open and closed/limiting station quantities when no choke cap is imposed, using the baseline calibration  $q_O = 1.06$  and  $q_C = 0.67$ . Solid segments are identified by the observed allocations and slope bounds; dashed segments are admissible extensions.

curve must kink and bend to hit the choke cap. In the higher-loss panel, the flat branch extrapolates to  $P(0) = 3.5 < 4$ , so no kink is required. This mainly trims the closed/limiting upper shadow-price bound at observed quantity (about  $2.67 \rightarrow 2.34$ ), lowering the upper welfare endpoint. We therefore present no-choke results as the headline interval and use the choke case as a disciplined robustness check.

Figure 7 summarizes this effect directly in shadow-price space. Horizontal bars show the admissible shadow-price intervals at observed quantities for each station type. Open-station ranges are nearly unchanged by the choke, while the closed/limiting upper bound contracts noticeably. This contraction is what disciplines the worst-case welfare calculation.

At baseline parameters ( $\bar{p} = 0.8$ ,  $\varepsilon \in [0.2, 0.4]$ ), the station-level *no-choke* joint robust bounds imply

$$\mathcal{L}_{Mis} / \mathcal{L}_{Harb} \in [1.13, 9.06].$$

Equivalently, with  $\mathcal{L}_{Harb} \approx 2.03\%$ , misallocation loss is bounded by  $\mathcal{L}_{Mis} \in [2.29\%, 18.36\%]$  of baseline spending. Imposing a choke cap  $M = 4$  leaves the lower endpoint unchanged and tightens the upper endpoint to  $\mathcal{L}_{Mis} = 12.62\%$  (ratio upper endpoint 6.23).

The depth of the price control affects the robust interval itself. Table 1 reports *no-choke* station-level intervals as  $\bar{p}$  varies. As  $\bar{p}$  falls (deeper price control), open stations expand demand and closed/limiting stations are more starved. At  $\bar{p} = 0.5$ , the ratio interval is  $\mathcal{R} \in [2.90, 23.20]$ ; at  $\bar{p} = 1.0$ , it is  $\mathcal{R} \in [0.41, 3.26]$ .

The key takeaway is that with rationing differences across stations, upper-bound misallocation losses can be many multiples of the Harberger triangle. The interval is wide in the two-market aggregation, but its upper end rises sharply as controls deepen. The heterogeneity across stations is the source of this additional welfare destruction.

The choke constraint  $P(0) \leq M$  illustrates how an additional global restriction re-

Station-Level Demand Curves Consistent with Observed Rationing (With Choke M=4) (displayed in per-station units)

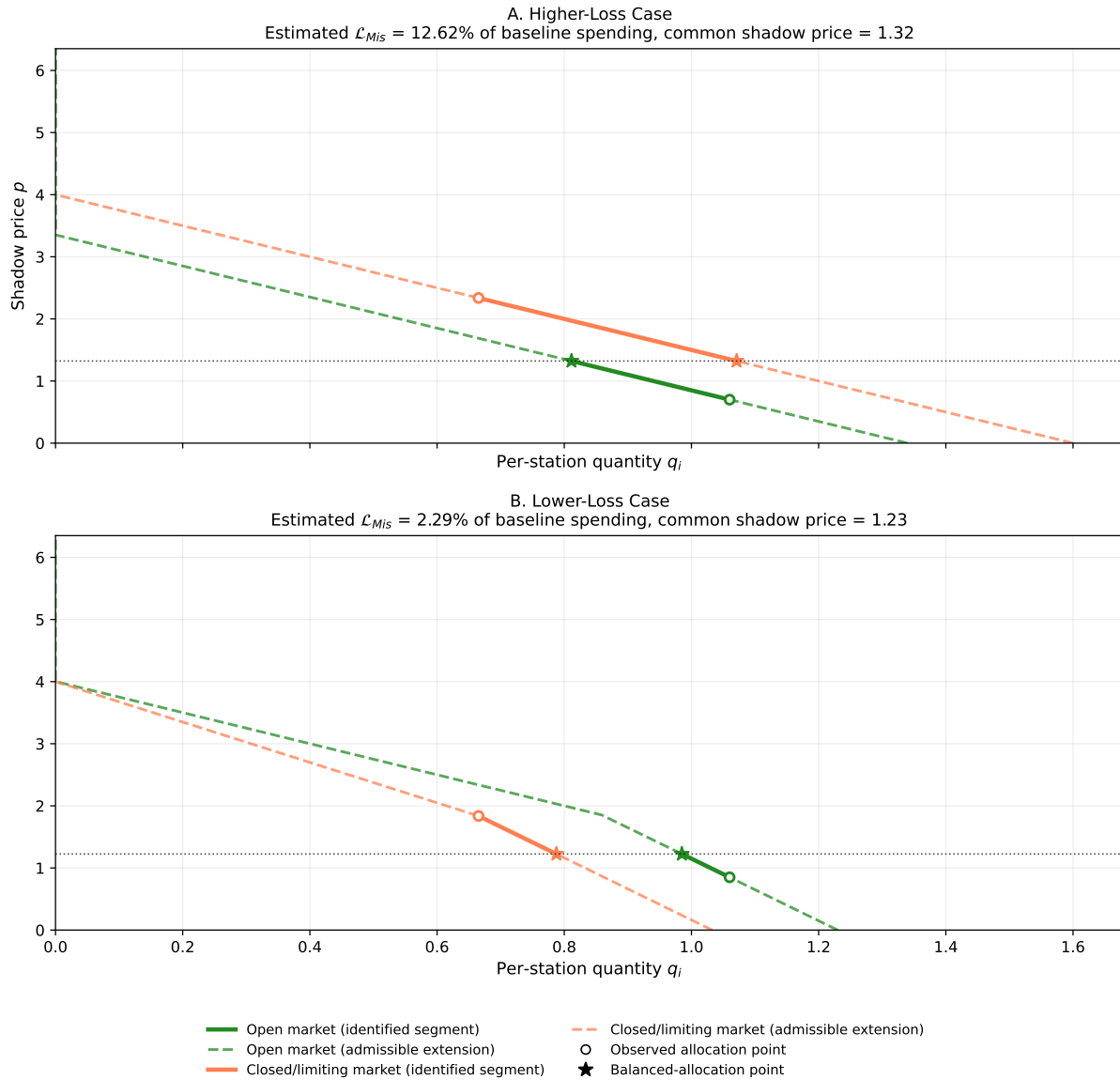


Figure 6: **Station-Level Demand Curves With Choke.** Same construction as Figure 5, using the same baseline calibration and now imposing  $P(0) \leq M = 4$ . The choke cap narrows admissible shadow-price ranges, which tightens the upper bound on misallocation losses.

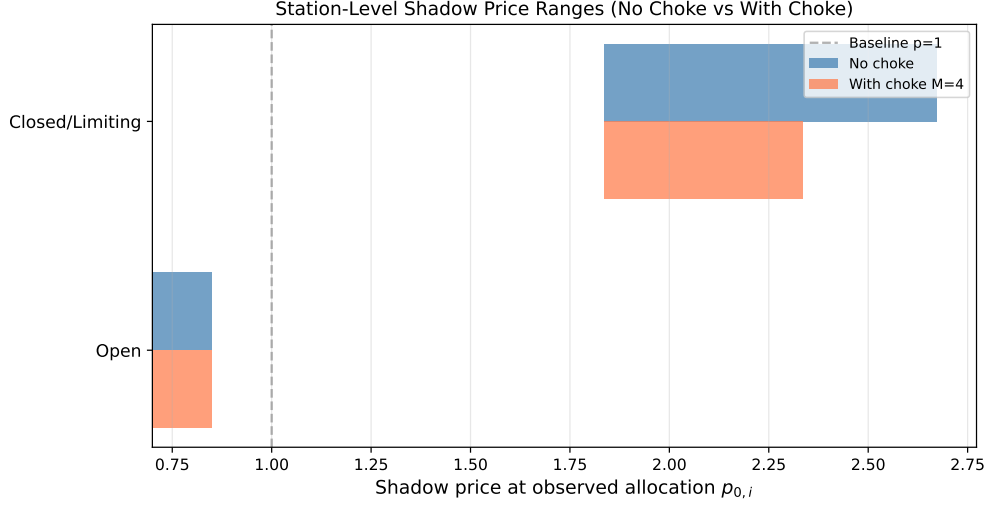


Figure 7: **Station-Level Shadow Price Ranges, With and Without Choke.** Horizontal bars show admissible shadow-price intervals at observed quantities for open and closed/limiting stations in the baseline calibration. Blue bars are no-choke ranges; orange bars impose  $P(0) \leq M = 4$ , which tightens the upper range for closed/limiting stations.

Table 1: Sensitivity to Controlled Price (Robust Intervals)

$\bar{p}$	$q_{open}$	$q_{closed}$	$\mathcal{L}_{Mis}$ interval (%)	$\mathcal{L}_{Harb}$ (%)	$\mathcal{R}$ interval
0.5	1.15	0.52	[5.87, 46.99]	2.03	[2.90, 23.20]
0.8	1.06	0.67	[2.29, 18.36]	2.03	[1.13, 9.06]
1.0	1.00	0.76	[0.83, 6.61]	2.03	[0.41, 3.26]

Notes: Open station quantity is demand at  $\bar{p}$ ; closed/limiting receive the residual so aggregate shortage equals 9%. Quantities  $(q_{open}, q_{closed})$  are baseline-calibration values (with  $\varepsilon = 0.3$ ), while welfare objects are reported as robust intervals. Intervals in this table are no-choke joint robust bounds over admissible station anchors. With choke  $M = 4$ , upper endpoints are lower (e.g., at  $\bar{p} = 0.8$ ,  $\mathcal{R}_{upper}$  falls from 9.06 to 6.23).

shapes the identified set. Without it, linear extrapolation from the anchor ( $q = 1, p = 1$ ) with steep slope  $g = -5$  implies  $P(0) = 6$  and  $P(0.665) \approx 2.67$  at closed/limiting stations. With  $M = 4$ , the curve must respect  $P(0) \leq 4$ , which trims the admissible upper shadow price at observed quantity to about 2.34. This is why the choke run lowers the upper welfare bound.

But the choke is essentially the *only* extra constraint doing work in the station-level analysis. Lemma 1 provides joint bounds on misallocation across  $n$  markets by optimizing over all demand functions consistent with slope bounds, anchor points, and a binding adding-up constraint  $\sum_i q_i = \bar{Q}$ . With only two aggregated station types, however, the adding-up constraint provides limited additional discipline. In the baseline calibration, open stations receive  $q_O = 1.06$  (admissible range  $[1.04, 1.08]$ ) and closed stations receive the residual  $q_C = 0.67$  (admissible range  $[0.63, 0.70]$ ); there is little cross-market tradeoff to exploit.

In this two-market aggregation, the upper bound is driven mainly by the admissible shadow-price wedge between open and closed markets, while adding-up mostly determines the residual split  $q_C = \bar{Q} - q_O$ . In practice, the slope bounds and the choke cap are doing most of the identifying work.

The station-level approach therefore illustrates the partial-identification logic but does not fully exploit Lemma 1's joint structure. Doing so requires finer market disaggregation where the adding-up constraint genuinely binds.

## 7.5 State-Level Robust Bounds

This section disaggregates the national market into 48 states (all states except Alabama and Alaska, which are missing from the AAA coverage). This is where adding-up becomes operational. In the two-market station split, one market is largely residual. In the 48-state system, no single state can absorb all adjustments: increasing quantity in one

state must be offset by reductions elsewhere to satisfy  $\sum_i q_i = \bar{Q}$ . That coupling is exactly what disciplines the bounds.

Using the station-level baseline calibration from Section 7.4 (with admissible ranges  $q_{open} \in [1.04, 1.08]$  and  $q_{non-open} \in [0.63, 0.70]$ ), we set  $q_{open} = 1.06$  and  $q_{non-open} = 0.655$  to map rationing shares into state quantities. For each state  $i$ , the data provide two inputs: a rationing share  $r_i$  (limiting plus out-of-fuel) and a weight  $w_i$  (share of national stations). The state's per-station quantity relative to baseline is

$$q_i^{rel} = (1 - r_i) \cdot q_{open} + r_i \cdot q_{non-open},$$

and its contribution to national quantity is  $q_i^{obs} = w_i \cdot q_i^{rel}$ . States with high rationing (Connecticut at 90%, Massachusetts at 93%) have low relative quantities; states with zero rationing (Idaho, Montana, Wyoming) receive  $q_{open}$ .

We observe quantities but not shadow prices directly. To construct bounds on shadow prices, we extrapolate from baseline. The baseline point ( $q_i^{base}, p^{base} = 1$ ) together with elasticity bounds  $\varepsilon \in [0.2, 0.4]$  implies slope bounds  $g_L = -5/q_i^{base}$  and  $g_U = -2.50/q_i^{base}$ . Linear extrapolation from baseline to the observed quantity gives

$$p_{0,i} \in \left[ p^{base} + g_L(q_i^{obs} - q_i^{base}), p^{base} + g_U(q_i^{obs} - q_i^{base}) \right].$$

For rationed states where  $q_i^{obs} < q_i^{base}$ , this interval lies above baseline; for states receiving above-baseline quantities, it lies below.

Figure 8 maps state shadow-price bounds at observed allocations, expressed relative to baseline price. The top panel shows the *upper bound*: the highest shadow price consistent with the baseline anchor and elasticity restrictions. The bottom panel shows the *lower bound*: the lowest shadow price consistent with those same restrictions. Red indicates higher inferred shadow prices relative to baseline; blue indicates lower inferred

shadow prices. States with high rationing generally appear in redder bins (often above baseline), while low-rationing states are typically closer to or below baseline. Figure 9 in the appendix reports the full interval bounds for each state.

Applying the joint bounds from Lemma 1 with the adding-up constraint  $\sum_i q_i = \bar{Q}$  binding and optimizing over all admissible shadow-price anchors yields

$$\underline{\mathcal{L}}_{Mis} = 0.52\%, \quad \overline{\mathcal{L}}_{Mis} = 4.81\%.$$

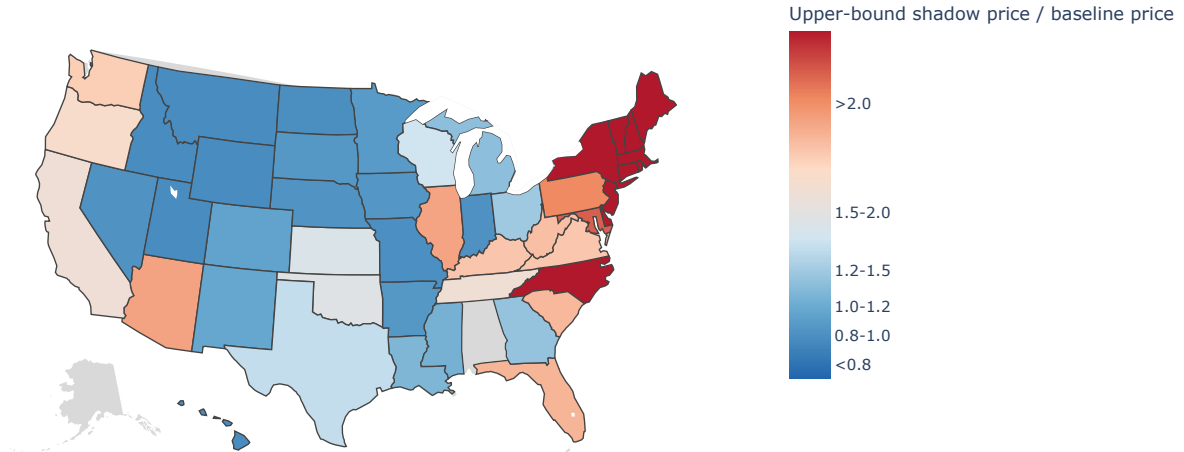
With a Harberger benchmark of  $\mathcal{L}_{Harb} = 2.03\%$  (using the steep elasticity bound  $\varepsilon = 0.2$ ), the misallocation ratio satisfies  $\mathcal{L}_{Mis} / \mathcal{L}_{Harb} \in [0.26, 2.38]$ .

The key object in this state exercise is an *adding-up-induced extremal*. For any candidate common shadow price  $p$ , each state has a feasible quantity interval  $q_i(p) \in [\ell_i(p), u_i(p)]$  implied by slope bounds and anchor restrictions. Without adding-up, the bound would choose each state's endpoint independently. With adding-up, the choices are coupled by  $\sum_i q_i(p) = \bar{Q}$ : increasing one state's quantity must be offset by reductions elsewhere. As a result, the extremal solution still pushes most states to interval endpoints, but must "peel off" some states from those endpoints just enough to satisfy national adding-up. This is exactly the mechanism that makes the state bounds tighter than a market-by-market envelope.

The state-level ratio lies in  $[0.26, 2.38]$ , compared to the station-level no-choke interval  $[1.13, 9.06]$ . The key reason is adding-up discipline across many markets. In the two-market station split,  $q_C = \bar{Q} - q_O$ , so adding-up is mostly bookkeeping. With 48 state markets, Lemma 1 imposes a genuinely joint problem: the optimizer must pick a common shadow price  $p^*$  and a vector  $(q_1, \dots, q_{48})$  that lies in all state-specific intervals and still satisfies  $\sum_i q_i = \bar{Q}$ . States with high rationing need increases to approach  $p^*$ , while low-rationing states must give up quantity. These offsetting reallocations limit how far the

Inferred State Shadow-Price Bounds Relative to Baseline (February 1974)

A. Upper Bound: Highest inferred shadow price (relative to baseline)



B. Lower Bound: Lowest inferred shadow price (relative to baseline)

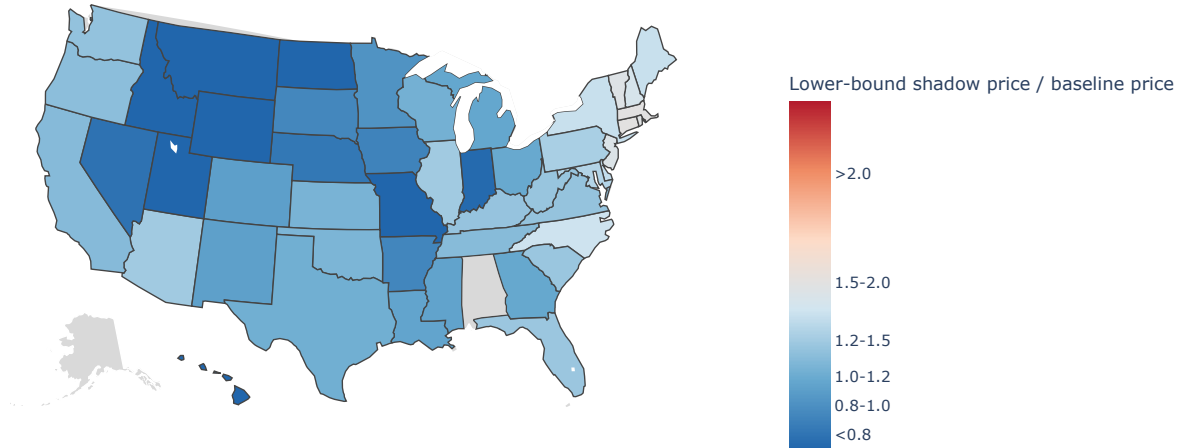


Figure 8: **State-Level Shadow-Price Bounds Relative to Baseline Price.** Colors show inferred shadow price divided by baseline price at each state's observed allocation. Panel A (top) reports the upper bound (highest value consistent with assumptions), and Panel B (bottom) reports the lower bound (lowest value consistent with assumptions). Red indicates higher inferred shadow prices; blue indicates lower inferred shadow prices.

worst-case shadow-price gap can be pushed.

There is a deeper reason for the gap. The state-level analysis treats each state as a single market with a single shadow price. This implicitly assumes efficient allocation *within* each state. Connecticut's 90% rationing share becomes a single average quantity; the analysis does not distinguish open stations in Hartford from closed stations in New Haven. The state-level bounds therefore capture only *across-state* misallocation, missing the within-state component entirely.

The station-level analysis makes no such assumption. It pools all open stations nationwide against all closed/limiting stations, wherever they are located. This captures total misallocation: both the gap between Connecticut and Idaho, and the gap between open and closed stations within Connecticut. The station-level ratio is higher because it measures more of the problem.

The comparison illustrates a general point: the measured misallocation ratio depends on the level of geographic aggregation. Aggregating to states imposes efficient within-state allocation and tightens the adding-up constraint across the 48 markets. Both forces moderate the worst-case bounds. The true misallocation lies somewhere in between, but the upper bounds at both levels confirm that misallocation costs can be several times larger than the Harberger triangle.

## 7.6 Misallocation beyond Geography

A barrel of crude can be refined into a slate of outputs—propane, butane, gasoline, jet fuel, heating oil, petrochemical feedstocks, and others. On the margin, tradeoffs exist: a given quantity of crude oil can yield more gasoline at the expense of less fuel oil, or vice versa. When prices are controlled product-by-product, these tradeoffs interact with small “nuisance” wedges (refining costs, accounting conventions, transportation frictions, and priority categories) to generate large shifts in the realized fuel mix. During the controls,

scarcity therefore appeared not only across space but across products. Propane shortages, diesel shortages, and heating-oil shortages rarely arrived as a single, stationary “energy shortage”; instead the binding constraint rotated across fuels as demand and costs moved, as the chaos theorem predicts.

A key mechanism was emphasized in 1973 testimony before the Joint Economic Committee<sup>7</sup>:

Phases 3 and 3A have created a number of price anomalies that frequently prevent the movement of products in proper directions, simply as a result of price considerations.

Heating oil illustrates both product-mix and temporal misallocation. Heating-oil prices were initially frozen at (low-demand) summer 1971 levels, weakening incentives to carry inventories into winter and to direct marginal refinery yield toward distillate. Shortages emerged in the winters of 1972–1973 and 1973–1974, contributing to school closures. Freezing prices led to freezing people. (Poole 1973; Verleger 1979; Deacon, Mead, and Agarwal 1980).

Input–output misallocation also arose outside fuels whenever controlled output prices met uncontrolled input costs (or vice versa). In the summer of 1973, chicken farmers gassed, drowned, and suffocated roughly a million baby chicks (TIME 1973; Times 1973; Press 1973). Retail chicken prices were controlled, but feed costs were not. That did not merely reduce poultry output; it blocked the price system from allocating supply across production stages. Raising chicks is an intertemporal, input–output segment—feed today becomes broilers weeks later. With revenues capped along that grow-out path, relatively small increases in feed costs pushed producers to a corner: abandon the “raise chicks into chickens” segment and liquidate immediately.

7. Testimony of James Emison, p. 205. The hearings contain extensive discussion of rotating shortages (U.S. Congress, Joint Economic Committee, Subcommittee on Consumer Economics 1973).

It's cheaper to drown em than to put em down and raise em," said Madison Clements of Waco (Press 1973).

The same temporal segmentation appeared in livestock: dairy farmers slaughtered cows and hog farmers culled breeding stock, temporarily increasing meat supply while reducing future flows of milk and pork. In each case, controls flattened relative returns across time and uses, so small cost wedges selected a vertex allocation—all supply routed to the “now” segment and essentially zero to the “later” segment.

Finally, supply-chain complexity amplified inefficiencies in the output mix. Allocation rules designated priority end uses, but policymakers underestimated input-output linkages. Oil production was prioritized, yet some upstream inputs were not. Propane, for instance, was essential for producing plastic piping used in oil extraction, but the plastics industry initially lacked priority designation. The resulting pipe shortages disrupted the very oil production that allocation policy sought to protect (Office 1974).

The misallocation generated by the price controls ran into political economy. Faced with shortage-chaos the political system was pushed toward direct quantity management. By the 1979 episode, for example, the DOE threatened yield regulations requiring refiners to produce a specified share of heating oil per barrel of crude and instructed refiners on inventory accumulation ahead of summer gasoline demand (Bradley 1997; Verleger 1979).

Allocation by fiat is a natural response to shortages because, as the chaos theorem indicates, once prices are prevented from doing their job, “the market” no longer selects a coherent allocation—it delivers corner outcomes with no welfare ordering. Price controls therefore tend to metastasize into quantity controls.<sup>8</sup>

8. Communism can be understood as universal price controls combined with full quantity allocation. A full analysis is beyond the scope of this paper, but the shortage economy that Kornai 1992 documented exhibited dynamics strikingly consistent with the chaos theorem. Soviet citizens carried avoska bags—from avos', meaning “perhaps” or “just in case”—because shortages were unpredictable: shoes today, soap to-

## 8 Conclusion

In markets without price controls, arbitrage pushes goods toward their highest-value uses, equalizing shadow prices across space, time, and sector. A binding price ceiling breaks this. Once money prices are frozen, the incentive to move goods to higher-value segments vanishes, and the efficient allocation becomes a knife-edge point inside a much larger feasible set.

The Chaos Theorem formalizes the consequence: equilibrium generically lands on corners where some markets are fully served and others receive nothing. Infinitesimal changes in nuisance parameters such as transportation costs can flip the economy between corner allocations, generating discontinuous welfare jumps from continuous parameter shifts. The patchwork of the 1973–74 gasoline crisis is not an accident but the generic outcome when prices cannot signal scarcity.

Our robust bounds analysis quantifies these welfare costs without parametric demand assumptions. Using only observed allocations, the ceiling price, and empirically plausible slope bounds, we find misallocation losses roughly 2 to 5 times the Harberger triangle; the quantity reduction accounts for under one-third of total welfare loss.

The same logic extends beyond geography. Heating-oil prices frozen at summer levels eliminated incentives to store winter inventories; controlled chicken prices with uncontrolled feed costs drove farmers to a corner on the input–output, intertemporal margin, leading them to destroy over a million chicks. Whenever controls suppress price variation across segments, seller indifference turns small cost wedges into large misallocations.

---

morrow, nothing next week. People joined any queue they encountered, often without knowing what was being sold, because the queue itself signaled temporary availability (Smith 1984). Production exhibited parallel irregularities. Factories "stormed"—alternating between slack periods when little was accomplished and frantic bursts of activity as plan deadlines approached (Filtzer 1996)—because input deliveries were erratic and uncoordinated with production schedules. The common mechanism was the absence of price signals to coordinate dispersed decisions, producing systemwide patterns of shortage and surplus that shifted unpredictably in response to small perturbations.

The shortage-chaos leads naturally to quantity controls.

The broader lesson is general: whenever a ceiling fragments an integrated market—gasoline, rental housing, agriculture, medical care—the main cost is not the familiar triangle, but the hidden misallocation behind it.

## A Omitted Proofs

### A.1 Theorem 1 Proof

*Proof of Theorem 1.* Because  $\tilde{W}_i(q_i) = \int_0^{q_i} P_i(x) dx$  is concave (as an integral of a nonincreasing function), the sum  $\tilde{W} = \sum_i \tilde{W}_i$  is concave on the convex polytope  $\mathcal{F}$ . A concave function attains its minimum at an extreme point, proving (i).

For (ii), fix a minimizer  $q^w \in \mathcal{F}$  of  $\tilde{W}$ . Since each  $P_i$  is continuous on  $[0, \bar{q}_i]$ ,  $\tilde{W}$  is continuously differentiable on  $F$ , with  $\frac{\partial \tilde{W}}{\partial q_i}(q) = P_i(q_i)$  for all  $q \in \mathcal{F}$ . The standard Karush-Kuhn-Tucker conditions apply: at  $q^w$ , there exist  $\lambda, \{\mu_i\}, \{\nu_i\}$  such that

$$\text{(stationarity)} \quad P_i(q_i^w) + \lambda - \mu_i + \nu_i = 0 \quad \text{for all } i, \quad (\text{A1})$$

$$\text{(complementary slackness)} \quad \mu_i q_i^w = 0, \quad \nu_i (q_i^w - \bar{q}_i) = 0 \quad \text{for all } i, \quad (\text{A2})$$

$$\text{(primal feasibility)} \quad \sum_i q_i^w = \bar{Q}, \quad 0 \leq q_i^w \leq \bar{q}_i \quad \text{for all } i, \quad (\text{A3})$$

$$\text{(dual feasibility)} \quad \mu_i, \nu_i \geq 0 \quad \text{for all } i. \quad (\text{A4})$$

We define  $\lambda_{\text{worst}} := -\lambda$  and observe that there three possible cases for each market  $i$ .

We go through them one-by-one.

**Case 1:**  $0 < q_i^w < \bar{q}_i$ . Both constraints  $-q_i \leq 0$  and  $q_i - \bar{q}_i \leq 0$  are slack at  $q^w$ , so by complementary slackness (A2) we must have  $\mu_i = 0 = \nu_i$ . We substitute these into (A1) to deduce  $P_i(q_i^w) = \lambda_{\text{worst}}$ .

**Case 2:**  $q_i^w = 0$ . Here the constraint  $q_i - \bar{q}_i \leq 0$  is slack (since  $q_i^w - \bar{q}_i < 0$ ), so  $\nu_i = 0$  by (A2), while  $\mu_i \geq 0$  is free. Equation (A1) becomes  $P_i(0) = \lambda_{\text{worst}} + \mu_i \geq \lambda_{\text{worst}}$ .

**Case 3:**  $q_i^w = \bar{q}_i$ . Now the constraint  $-q_i \leq 0$  is slack (since  $-q_i^w = -\bar{q}_i < 0$ ), so  $\mu_i = 0$  by (A2), while  $\nu_i \geq 0$  is free. Equation (A1) becomes  $P_i(\bar{q}_i) = \lambda_{\text{worst}} - \nu_i \leq \lambda_{\text{worst}}$ .

As each  $P_i(\cdot)$  is weakly decreasing and nonnegative, necessarily  $\lambda_{\text{worst}} \geq 0$ .

Part (iii) follows immediately: for a single-market allocation with  $q_j = \bar{Q}$  and  $q_{k \neq j} = 0$ , we have  $\tilde{W} = \int_0^{\bar{Q}} P_j(x) dx$ , so minimizing across  $j$  yields the stated criterion. ■

## A.2 Chaos Theorem

This appendix provides the technical machinery for Theorem 2.

Let  $\theta \in \Theta \subset \mathbb{R}^m$  be a compact, nonempty parameter space. There are sub-markets  $i = 1, \dots, n$  with inverse demands  $P_i(x; \theta)$ . We assume i) for each  $i$  and every  $\theta$ , the map  $x \mapsto P_i(x; \theta)$  is continuous and strictly decreasing; and ii) for each  $x$ , the map  $\theta \mapsto P_i(x; \theta)$  is continuous. We also assume iii) sub-market unit costs  $c_i(\theta)$  and the total quantity  $\bar{Q}(\theta) > 0$  are continuous in  $\theta$ .

The feasible splits  $q = (q_1, \dots, q_n)$  satisfy  $\sum_{i=1}^n q_i = \bar{Q}(\theta)$  and  $q_i \geq 0$ . We define

$$W(q; \theta) = \sum_{i=1}^n \int_0^{q_i} P_i(x; \theta) dx.$$

Consider

$$\max_{q \geq 0} \sum_{i=1}^n \int_0^{q_i} P_i(x; \theta) dx - \sum_{i=1}^n c_i(\theta) q_i \quad \text{s.t.} \quad \sum_{i=1}^n q_i = \bar{Q}(\theta).$$

As each  $P_i(\cdot; \theta)$  is strictly decreasing, the objective is strictly concave in  $q$ , hence the maximizer  $q^*(\theta)$  is unique. The feasible correspondence

$$\Gamma(\theta) := \left\{ q \in \mathbb{R}_+^n : \sum_i q_i = \bar{Q}(\theta) \right\},$$

has compact values and a closed graph by the continuity of  $\bar{Q}$ . The objective is continuous in  $(q, \theta)$  (by the joint continuity of  $P_i$  and continuity of  $c_i$  and  $\bar{Q}$ ). Therefore, by Berge's Maximum Theorem, both the unique maximizer  $\theta \mapsto q^*(\theta)$  and the value function

$$\theta \mapsto \sum_{i=1}^n \int_0^{q_i^*(\theta)} P_i(x; \theta) dx - \sum_{i=1}^n c_i(\theta) q_i^*(\theta),$$

are continuous in  $\theta$ . On any region where the optimizer is interior, the multiplier  $\theta \mapsto \lambda(\theta)$  is also continuous, as  $\lambda(\theta) = P_i(q_i^*(\theta); \theta) - c_i(\theta)$ .

Now suppose we have a binding ceiling  $\bar{p}$ . Define  $\bar{q}_i(\theta) := D_i(\bar{p}; \theta)$  and aggregate

quantity  $\bar{Q}(\theta) := S(\bar{p}; \theta)$ . The feasible set is

$$\mathcal{F}(\theta) = \left\{ q \in \mathbb{R}_+^n : \sum_{i=1}^n q_i = \bar{Q}(\theta), 0 \leq q_i \leq \bar{q}_i(\theta) \forall i \right\}.$$

We make the genericity assumptions

- I.  $0 < \bar{Q}(\theta) < \sum_{i=1}^n \bar{q}_i(\theta)$ ;
- II.  $\bar{Q}(\theta) \neq \sum_{i \in S} \bar{q}_i(\theta)$  for every  $S \subset \{1, \dots, n\}$ ;
- III.  $c_i(\theta) \neq c_j(\theta)$  for  $i \neq j$ .

We solve

$$\min_{q \in \mathcal{F}(\theta)} c(\theta) \cdot q.$$

We order costs as  $c_{(1)}(\theta) < \dots < c_{(n)}(\theta)$  and let  $k$  denote the unique index with  $\sum_{s=1}^{k-1} \bar{q}_{(s)}(\theta) < \bar{Q}(\theta) < \sum_{s=1}^k \bar{q}_{(s)}(\theta)$ . Then the unique optimizer is

$$q_{(r)}^*(\theta) = \begin{cases} \bar{q}_{(r)}(\theta), & r < k, \\ \bar{Q}(\theta) - \sum_{s=1}^{k-1} \bar{q}_{(s)}(\theta), & r = k, \\ 0, & r > k, \end{cases}$$

i.e., we “fill in increasing  $c$ ” with at most one partial coordinate. Changing  $\theta$  that breaks a cost tie ( $c_i(\theta) = c_j(\theta)$ ) that changes which markets are filled causes a discrete jump in allocations.

We suppress dependence on the parameter  $\theta$  and recall the optimization problem, linear program

$$\min \{c \cdot q : q \in \mathcal{F}\}. \quad (\star)$$

For the local instability argument we fix the feasible polytope  $\mathcal{F} = \mathcal{F}(\theta^*)$  and consider perturbations that act only through the cost vector  $c(\theta)$ . Thus, we treat  $c$  as the effective parameter in  $(\star)$ . We maintain Assumptions I. and II. Assumption II. means that every vertex  $v$  of  $\mathcal{F}$  has exactly one coordinate strictly between its bounds (the partial coordinate), and all other coordinates are at 0 or at  $\bar{q}_i$ . To elaborate, a point  $v \in \mathcal{F}$  is a vertex iff exactly  $n - 1$   $q_i \in \{0, \bar{q}_i\}$ , with the equality  $\sum q_i = \bar{Q}$  then fixing the partial coordinate.

We say that two distinct vertices  $v$  and  $w$  are *adjacent* if they share an edge: along the

edge exactly the pair  $(r, s)$  of coordinates moves (with all others fixed at bounds) and

$$w - v = \Delta(e_s - e_r) \quad \text{for some } r \neq s \text{ and } \Delta \neq 0, \quad (1)$$

where  $r$  is the unique partial index at  $v$  (so  $0 < v_r < \bar{q}_r$ ); and at  $w$ , one of  $r$  or  $s$  is the new partial (non-bound coordinate) and the other hits a bound. Equivalently, edges are exactly the one-dimensional faces on which two coordinates are free (subject to the sum constraint), and the others are fixed at bounds.

For any  $v \in \mathcal{F}$ , the (outer) normal cone is

$$\mathcal{N}_v = \{c \in \mathbb{R}^n : c \cdot (x - v) \geq 0 \forall x \in F\}.$$

The following is standard:

**Remark 4.**  $v$  solves  $(\star)$  if and only if  $c \in \mathcal{N}_v$ .

Moreover,

**Remark 5.** If a given  $c$  makes exactly two distinct vertices  $v, w$  optimal, then  $v, w$  are adjacent and  $c \cdot (w - v) = 0$ .

Denote the set of such common-optimal costs by

$$\mathcal{H}_{vw} := \mathcal{N}_v \cap \mathcal{N}_w \cap \{c : c \cdot (w - v) = 0\}.$$

We say that  $c^*$  is a *simple tie* for  $v, w$  if

$$c^* \in \text{relint}(\mathcal{H}_{vw}) \quad \text{and} \quad c^* \notin \mathcal{N}_u \text{ for any other vertex } u.$$

Note that if  $c$  makes  $v$  and  $w$  optimal but the tie is not simple, then every neighborhood of  $c$  contains some  $\hat{c}$  that is a simple tie for  $v, w$ ; thus Lemma 2 still yields crossings arbitrarily close to any  $(v, w)$  tie.

**Lemma 2.** *Let  $v \neq w$  be adjacent vertices and  $c^*$  a simple tie for  $v, w$ . Then for any neighborhood  $U \subset \mathbb{R}^n$  of  $c^*$  there exists  $\varepsilon > 0$  and a continuously-differentiable function  $c : [-\varepsilon, \varepsilon] \rightarrow U$  such that the unique optimizer of  $(\star)$  equals  $v$  for  $t < 0$  and  $w$  for  $t > 0$ , while at  $t = 0$  both  $v$  and  $w$  are optimal.*

*Proof.* As  $c^* \in \text{relint } \mathcal{H}_{vw}$  and no third cone meets at  $c^*$ , there exists  $\rho > 0$  with  $B(c^*, \rho) \cap \text{fan}(\mathcal{F}) = \text{int } \mathcal{N}_v \dot{\cup} \mathcal{H}_{vw} \dot{\cup} \text{int } \mathcal{N}_w$  ( $\dot{\cup}$  denotes the disjoint union). Thus, for any  $\eta$  with  $(w -$

$v) \cdot \eta < 0$ , the line  $c(t) = c^* + t\eta$  (for  $|t|$  small) satisfies  $(w - v) \cdot c(t) = t(w - v) \cdot \eta$  and thus crosses  $\mathcal{H}_{vw}$  with a sign change, so  $c(t) \in \text{int } \mathcal{N}_v$  for  $t < 0$ ,  $c(0) \in \mathcal{H}_{vw}$ , and  $c(t) \in \text{int } \mathcal{N}_w$  for  $t > 0$ . Optimality follows from Remark 4. ■

We continue to let  $v, w$  be adjacent vertices with  $w - v = \Delta(e_s - e_r)$ ,  $\Delta \neq 0$ , as in (1). Let  $c(t)$  be a continuously-differentiable function as in Lemma 2. Define the welfare jump at the crossing by

$$\Delta W = \lim_{t \downarrow 0} W(w; c(t)) - \lim_{t \uparrow 0} W(v; c(t)).$$

The next lemma reassures us that the  $-c \cdot q$  contribution cancels in the limit, as  $c(\cdot)$  is continuous at 0 and  $c(0) \cdot (w - v) = 0$ .

**Lemma 3.** *We have*

$$\Delta W = \int_{v_s}^{w_s} P_s(x) dx - \int_{w_r}^{v_r} P_r(x) dx. \quad (2)$$

*Proof.* By definition,

$$\begin{aligned} \Delta W &= \lim_{t \downarrow 0} \left( \sum_i \int_0^{w_i} P_i(x) dx - c(t) \cdot w \right) - \lim_{t \uparrow 0} \left( \sum_i \int_0^{v_i} P_i(x) dx - c(t) \cdot v \right) \\ &= \sum_i \left( \int_0^{w_i} P_i - \int_0^{v_i} P_i \right) - \lim_{t \rightarrow 0} c(t) \cdot (w - v) \\ &= \sum_i \int_{v_i}^{w_i} P_i - c(0) \cdot (w - v) = \int_{v_s}^{w_s} P_s - \int_{w_r}^{v_r} P_r, \end{aligned}$$

where we used the definition of a simple tie and Remark 5 to eliminate  $c(0) \cdot (w - v) = 0$ . ■

## Proof of Theorem 2

*Proof of Theorem 2.* By Lemma 2, we can construct a smooth crossing  $c(\cdot)$ . By Lemma 3,  $\Delta W[c] = \int_{v_s}^{w_s} P_s - \int_{w_r}^{v_r} P_r$ , which is nonzero by hypothesis ( $\Delta W \neq 0$ ).

Define the reversed crossing  $\tilde{c}(t) := c(-t)$ . The optimizer flips in the opposite direction, and  $\Delta W[\tilde{c}] = -\Delta W[c]$ , with the same magnitude  $|\Delta W|$ .

Setting  $c_+ := c$  and  $c_- := \tilde{c}$  yields the two paths with welfare jumps  $+|\Delta W|$  and  $-|\Delta W|$  respectively. Since these have opposite signs, welfare is not locally monotone in any neighborhood of  $c^* \equiv c(\theta^*)$ . ■

*Proof of Corollary 1.* For every neighborhood  $U$  of  $c^* \equiv c(\theta^*)$ , Lemma 2 provides  $c^-, c^+ \in U$  with  $q^*(c^-) = v$  and  $q^*(c^+) = w$ . Then

$$\|q^*(c^+) - q^*(c^-)\|_1 = \|w - v\|_1 = |\Delta| + |-\Delta| = 2\Delta > 0. \quad \blacksquare$$

### A.3 Lemma 1 Proof

*Proof.* First we observe that for all  $P \in \mathcal{P}$  with shadow price  $p^* = p^*(P)$  and optimizer  $q^*$ ,

$$\Phi(P) = \bar{Q} p^* - \sum_{i=1}^n q_i^{\text{obs}} p_{0,i} - \sum_{i=1}^n \int_{p_{0,i}}^{p^*} q_i(p) dp \quad (3)$$

To see this, observe that for any monotone  $P_i$  and any  $a < b$ ,

$$\int_a^b P_i(q) dq = bP_i(b) - aP_i(a) - \int_{P_i(a)}^{P_i(b)} q_i(p) dp,$$

We plug in  $a = q_i^{\text{obs}}$ ,  $b = q_i^*$ , and subtract  $p^*(q_i^* - q_i^{\text{obs}})$  to get

$$\int_{q_i^{\text{obs}}}^{q_i^*} (P_i - p^*) dq = q_i^* (P_i(q_i^*) - p^*) - q_i^{\text{obs}} p_{0,i} - \int_{p_{0,i}}^{P_i(q_i^*)} q_i(p) dp + p^* q_i^{\text{obs}}.$$

If  $0 < q_i^* < q_i^{\text{max}}$ , then  $P_i(q_i^*) = p^*$  and the first term vanishes. If  $q_i^* = q_i^{\text{max}}$ , then  $P_i(q_i^*) = P_i(q_i^{\text{max}}) \geq p^*$  and, as  $q_i(p) = q_i^{\text{max}}$  for  $p \leq P_i(q_i^{\text{max}})$ , we get

$$q_i^{\text{max}} (P_i(q_i^{\text{max}}) - p^*) - \int_{p^*}^{P_i(q_i^{\text{max}})} q_i(p) dp = \int_{p^*}^{P_i(q_i^{\text{max}})} (q_i^{\text{max}} - q_i(p)) dp = 0.$$

If  $q_i^* = 0$ , then  $P_i(0) \leq p^*$  and  $q_i(p) = 0$  for  $p \in (P_i(0), p^*]$ , so extending the upper limit of  $\int_{p_{0,i}}^{P_i(0)} q_i$  to  $p^*$  adds zero. Summing over  $i$  yields (3).

Consequently, for fixed  $p$  the dependence on the  $q_i(\cdot)$ s is through the linear functionals

$$- \sum_{i: p \geq p_{0,i}} \int_{p_{0,i}}^p q_i(s) ds + \sum_{i: p < p_{0,i}} \int_p^{p_{0,i}} q_i(s) ds,$$

subject to  $q_i(s) \in [\ell_i(s), u_i(s)]$  for a.e.  $s$  and  $\sum_i q_i(p) = \bar{Q}$  at  $s = p$ . Thus, for a.e.  $s \neq p$ , the linear objective is optimized at an endpoint  $q_i(s) \in \{\ell_i(s), u_i(s)\}$ . At  $s = p$ , we may select a point in the intersection of the hyperplane  $\{q: \sum_i q_i = \bar{Q}\}$  with the set  $\times_i [\ell_i(p), u_i(p)]$ ;

viz., at most one interior coordinate suffices. The endpoint that maximizes (minimizes) is  $\ell_i(u_i)$  when  $p \geq p_{0,i}$  and  $u_i(\ell_i)$  when  $p < p_{0,i}$ . ■

#### A.4 Theorem 3 Proof

*Proof.* Fix an optimizer  $p$  of (1) (the lower-bound procedure is analogous). Lemma 1 pins down the  $q_i(\cdot)$ s: on  $[\min\{p, p_{0,i}\}, \max\{p, p_{0,i}\}]$ , we set  $q_i(s) = \ell_i(s)$  or  $u_i(s)$  as prescribed; and at  $s = p$ , we pick a split  $\sum_i q_i(p) = \bar{Q}$  within  $\times_i [\ell_i(p), u_i(p)]$ . Outside  $[\min\{p, p_{0,i}\}, \max\{p, p_{0,i}\}]$ , we choose one endpoint everywhere (prices outside of these ranges don't affect the objective). Each  $q_i(\cdot)$  is nonincreasing and piecewise affine in  $s$ , with slope  $1/g_{i,L}$  or  $1/g_{i,U}$ . We invert these piecewise to define  $P_i^*$ : an affine  $s \mapsto q_i(s)$  with slope  $1/g$  becomes an affine  $q_i \mapsto P_i(q_i)$  with slope  $g \in \{g_{i,L}, g_{i,U}\}$ .  $P_i^*(q_i^{\text{obs}}) = p_{0,i}$  holds by construction, and we guarantee  $P_i^*(0) \leq M_i$  by assigning the least-negative slope,  $g_{i,U}$ , to  $P_i^*$  near  $q_i = 0$  if needed. This  $P^* \in \mathcal{P}$  attains the inner optimum at  $p$ , hence, the global bound. ■

## B Additional Robustness Figures

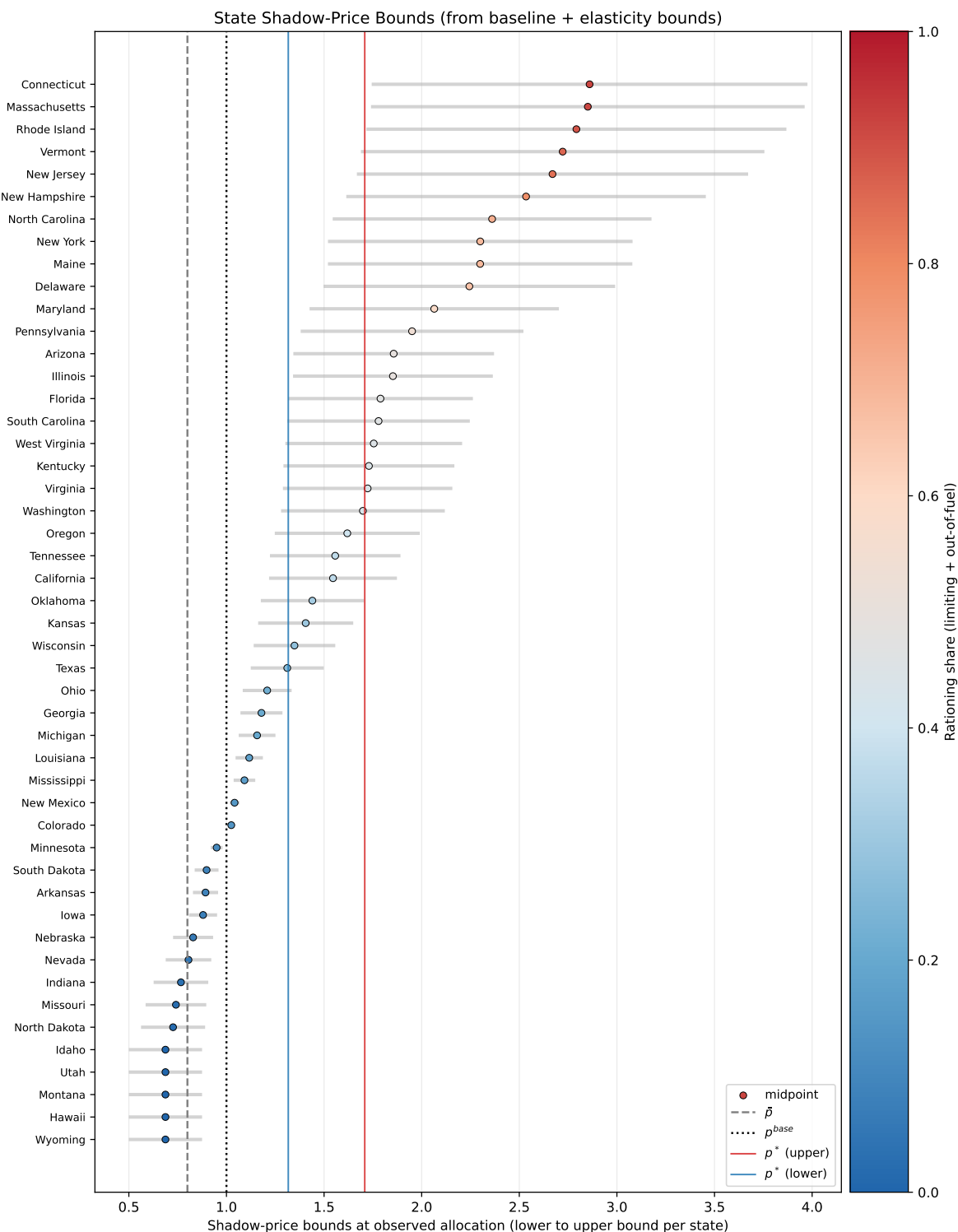


Figure 9: **State-Level Shadow-Price Bounds by State.** Each gray horizontal segment shows a state's admissible shadow-price interval at its observed allocation. The dot marks the interval midpoint and is colored by rationing share (higher rationing corresponds to higher values on the color scale). Dashed/dotted vertical lines mark the controlled and baseline prices; solid vertical lines mark the common shadow prices from the upper- and lower-bound joint solutions.

## C Hill Model Calibration and Robustness

This appendix provides an alternative to the robust bounds approach using a parametric Hill (sigmoidal) demand specification. The Hill functional form accommodates corner solutions where some markets receive zero allocation, which the standard CES specification cannot handle (as quantity approaches zero, CES shadow prices explode to infinity).

### C.1 Hill Demand Specification

The Hill functional form is:

$$P(q) = \frac{P_{\max}}{1 + (q/\kappa)^\eta}$$

This specification has three key properties. First,  $P(0) = P_{\max}$  is finite: the choke price represents maximum willingness to pay when facing complete stockout. Second,  $P(\kappa) = P_{\max}/2$ , so  $\kappa$  is the half-max quantity. Third, as  $q \rightarrow \infty$ ,  $P \rightarrow 0$ .

We calibrate the Hill function to match CES demand locally at the baseline  $(Q^{base}, p^{base}) = (1, 1)$ . This requires two conditions: (i)  $P(Q^{base}) = p^{base}$ , and (ii) the local elasticity at baseline equals  $\varepsilon$ . Solving these yields:

$$\eta = \frac{P_{\max}/p^{base}}{\varepsilon(P_{\max}/p^{base} - 1)}, \quad \kappa = Q^{base} \cdot (P_{\max}/p^{base} - 1)^{-1/\eta}$$

This calibration ensures the Hill and CES curves are tangent at baseline, with identical slope  $-p^{base}/(\varepsilon \cdot Q^{base})$ .

### C.2 Baseline Results

We calibrate the model as follows. The fraction of closed/limiting stations is  $s = 0.38$ , combining the 10% closed and 28% limiting categories from the AAA data. The aggregate shortage is  $\delta = 0.09$ , consistent with national estimates. The choke price ratio is  $P_{\max}/p^{base} = 5$ . The demand elasticity is  $\varepsilon = 0.25$ , consistent with estimates (Hughes, Knittel, and Sperling 2008). The controlled price is  $\bar{p} = 0.8$ , representing a 20% gap between the controlled price and what would have cleared the market. This is consistent with Frech and Lee (1987): given their 9% shortage and a short-run elasticity of 0.25, the market-clearing price would be approximately 36% above the pre-crisis level, implying a controlled-to-clearing ratio of roughly 0.8. .

At  $\bar{p} = 0.8$ , the Hill model implies demand per station of  $Q(0.8) = 1.056$ —customers want 5.6% more than at baseline. Open stations satisfy this elevated demand. Closed/limiting stations receive the residual:  $q_C^{obs} = (0.91 - 0.62 \times 1.056)/0.38 = 0.672$ , or 67% of baseline consumption.

Table 2 reports baseline findings. Under efficient allocation, open stations receive  $q_O^* = 0.564$  and closed/limiting stations receive  $q_C^* = 0.346$ , with a common shadow price of 1.43. Under the observed allocation, open stations consume more ( $q_O^{obs} = 0.655$ ) while closed/limiting stations consume less ( $q_C^{obs} = 0.255$ ). The shadow price gap is substantial: 0.80 at open stations versus 3.23 at closed/limiting stations.

Table 2: Hill Model: Baseline Results ( $\varepsilon = 0.25$ ,  $s = 0.38$ ,  $\bar{p} = 0.8$ ,  $P_{\max}/p^{base} = 5$ )

	Efficient	Observed
$q_O$ (open, aggregate)	0.564	0.655
$q_C$ (closed/limiting, aggregate)	0.346	0.255
$q_O$ per station	0.910	1.056
$q_C$ per station	0.910	0.672
Shadow price (O)	1.43	0.80
Shadow price (C)	1.43	3.23
Total Welfare	3.660	3.553
$\mathcal{L}_{Harb}$		0.018
$\mathcal{L}_{Mis}$	0	0.107
Ratio $\mathcal{R}$	0	5.85

The misallocation ratio is  $\mathcal{R} = 5.85$ : misallocation destroys nearly six times more welfare than the Harberger triangle. The magnitude reflects the asymmetry in allocation. Open stations consume 5.6% above baseline while closed/limiting stations receive only 67% of baseline—a ratio of roughly 1.6:1. This gap, combined with the curvature of demand, generates substantial welfare losses.

### C.3 Sensitivity to Controlled Price

The depth of the price control matters. Figure 10 shows how results vary with the controlled price  $\bar{p}$ . As  $\bar{p}$  falls (deeper price control), open stations expand their demand more aggressively, leaving less for closed/limiting stations. At  $\bar{p} = 0.5$ , open stations demand 17.6% above baseline, closed/limiting receive only 47.6% of baseline, and the misallocation ratio rises to  $\mathcal{R} = 19.4$ . At  $\bar{p} = 0.9$ , open stations demand 2.6% above baseline,

closed/limiting receive 72% of baseline, and  $\mathcal{R} = 3.7$ .

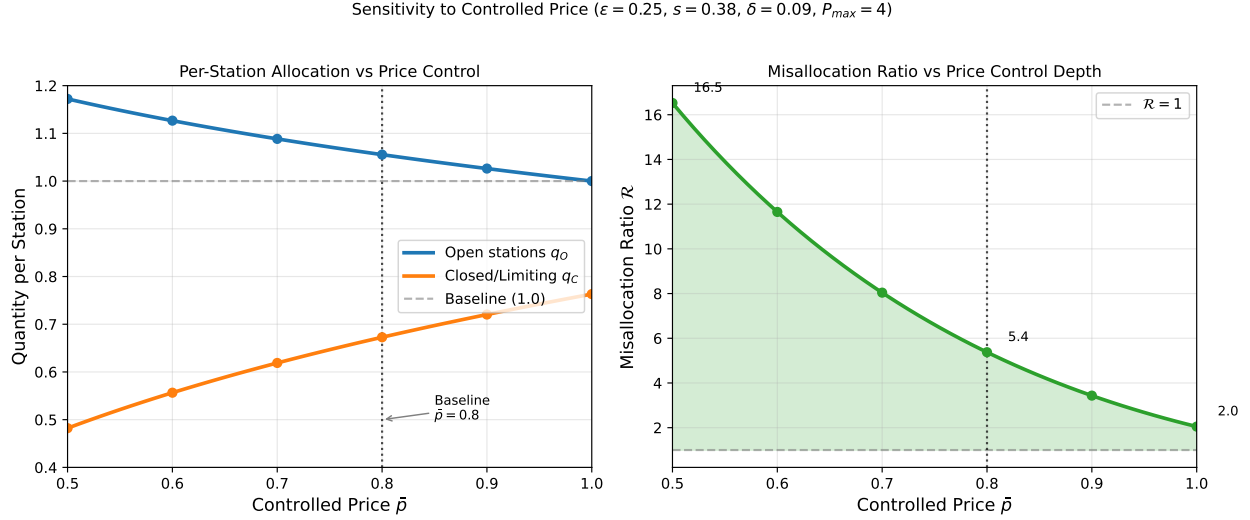


Figure 10: Sensitivity to controlled price  $\bar{p}$ . Left: Per-station allocation for open and closed/limiting stations. Right: Misallocation ratio  $\mathcal{R}$ . All specifications use  $\varepsilon = 0.25$ ,  $s = 0.38$ ,  $\delta = 0.09$ , and  $P_{\max}/p^{base} = 5$ .

## C.4 Sensitivity to Choke Price

The choke price  $P_{\max}$  governs how much consumers would pay to avoid complete exclusion. Figure 11 shows how the misallocation ratio varies with this parameter across different elasticity values. At our baseline elasticity ( $\varepsilon = 0.25$ ), the baseline calibration at  $P_{\max} = 5$  implies  $\mathcal{R} \approx 5.9$ , and the figure shows how this ratio changes as the choke price moves.

Figure 12 maps the full parameter space, showing  $\mathcal{R}$  as a function of both elasticity and choke price. The contours reveal that misallocation dominates Harberger losses across most of the empirically relevant region.

The robustness across this parameter space strengthens the core finding. Whether calibrated conservatively or aggressively, the Hill model consistently shows misallocation losses larger than Harberger triangles. At baseline, the Hill calibration gives  $\mathcal{R} \approx 5.9$ , compared with  $\mathcal{R} \approx 3.7$  for the robust piecewise-demand benchmark with choke, reflecting the Hill model's stronger curvature near  $q = 0$ . Both approaches support the qualitative conclusion that misallocation losses substantially exceed Harberger triangles.

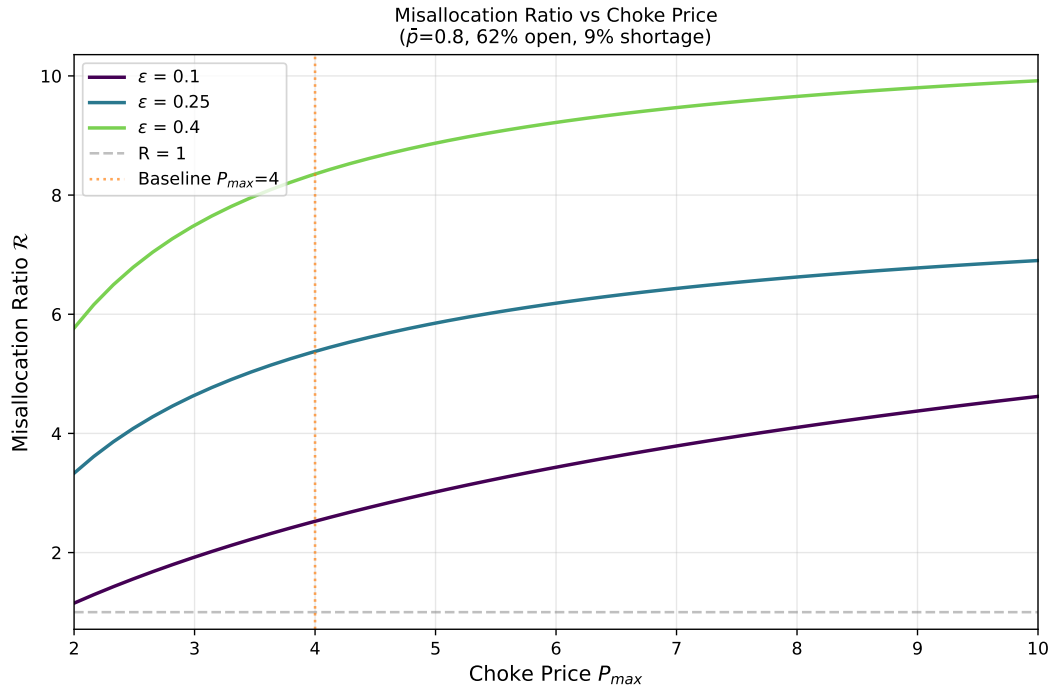


Figure 11: Misallocation ratio as a function of choke price ratio  $P_{max}/p^{base}$  for different demand elasticities.

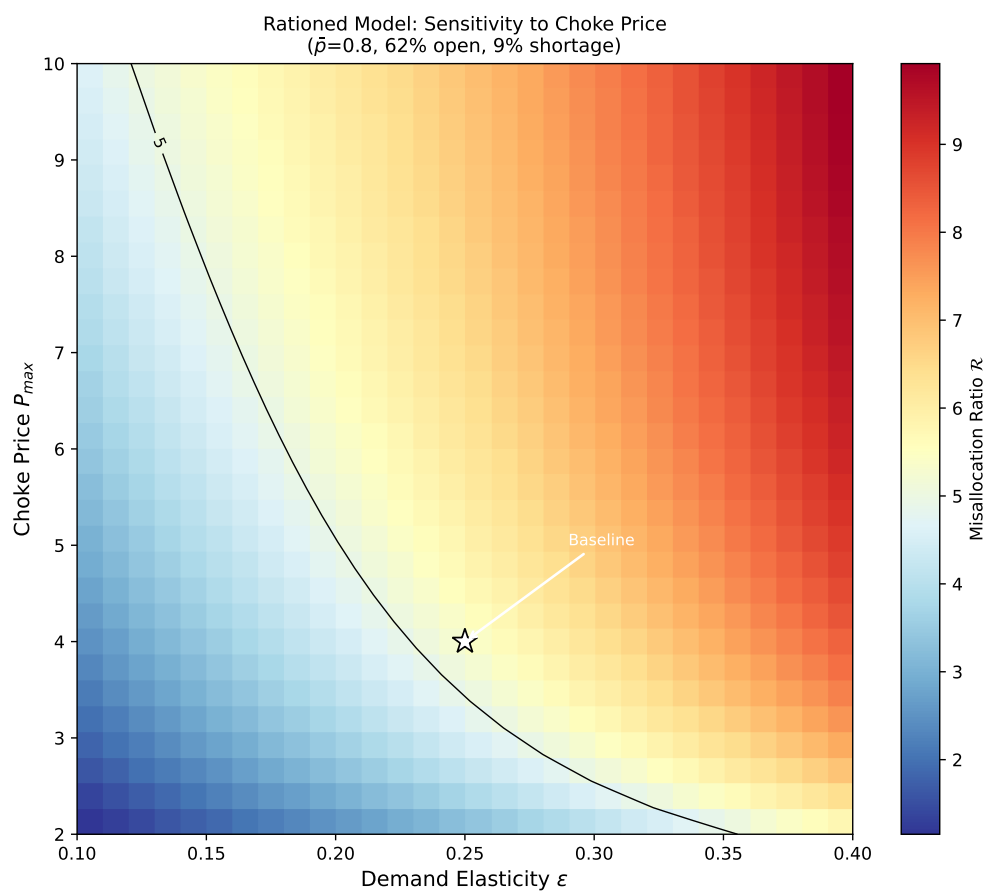


Figure 12: Sensitivity of misallocation ratio to demand elasticity and choke price. The star marks baseline parameters ( $\varepsilon = 0.25$ ,  $P_{\max} = 5$ ).

## References

- Akbarpour, Mohammad, Piotr Dworczak, and Scott Duke Kominers. 2024. "Redistributive Allocation Mechanisms." *Journal of Political Economy* 132 (6): 1831–1875.
- Barzel, Yoram. 1974. "A Theory of Rationing by Waiting." *Journal of Law and Economics* 17 (1): 73–95.
- Bradley, Robert L. 1997. *Oil, Gas and Government: The U.S. Experience*. Rowman & Littlefield Inc, October. ISBN: 0-8476-8108-4.
- Brunt, Christopher S. 2025. "Moving beyond Harberger's Triangle to present the inefficiency from misallocated market transactions under price controls" [in en]. *The Journal of Economic Education* 56, no. 4 (October): 322–328. ISSN: 0022-0485, 2152-4068, accessed December 26, 2025. <https://doi.org/10.1080/00220485.2025.2524631>. <https://www.tandfonline.com/doi/full/10.1080/00220485.2025.2524631>.
- Bulow, Jeremy I., and Paul D. Klemperer. 2012. "Regulated Prices, Rent Seeking, and Consumer Surplus." *Journal of Political Economy* 120 (1): 160–186. Accessed March 9, 2018.
- Buurma-Olsen, Jennifer, Hans R. A. Koster, Jos van Ommeren, and Jort Sinninghe Damsté. 2025. "Quantifying misallocation of public housing." *Journal of Public Economics* 242 (February): 105272. ISSN: 0047-2727, accessed January 14, 2026. <https://doi.org/10.1016/j.jpubeco.2024.105272>. <https://www.sciencedirect.com/science/article/pii/S0047272724002081>.
- Condorelli, Daniele. 2013. "Market and Non-Market Mechanisms for the Optimal Allocation of Scarce Resources." *Games and Economic Behavior* 82:582–591.
- Davis, Lucas W., and Lutz Kilian. 2011. "The Allocative Cost of Price Ceilings in the U.S. Residential Market for Natural Gas" [in en]. *Journal of Political Economy* 119, no. 2 (April): 212–241. ISSN: 0022-3808, 1537-534X, accessed May 15, 2025. <https://doi.org/10.1086/660124>. <https://www.journals.uchicago.edu/doi/10.1086/660124>.
- Deacon, Robert T., Walter J. Mead, and Vinod B. Agarwal. 1980. "Price Controls and International Petroleum Product Prices." Publisher: Department of Energy.
- Deacon, Robert T., and Jon Sonstelie. 1985. "Rationing by Waiting and the Value of Time: Results from a Natural Experiment." *Journal of Political Economy* 93 (4): 627–647.
- . 1989. "The Welfare Costs of Rationing by Waiting." *Economic Inquiry* 27:179–196.
- Diamond, Rebecca, Tim McQuade, and Franklin Qian. 2019. "The Effects of Rent Control Expansion on Tenants, Landlords, and Inequality: Evidence from San Francisco." *American Economic Review* 109 (9): 3365–3394. <https://doi.org/10.1257/aer.20181289>.

- Filtzer, Donald. 1996. "Labor Discipline, the Use of Work Time, and the Decline of the Soviet System, 1928-1991." *International Labor and Working-Class History*, no. 50, 9–28. ISSN: 0147-5479, accessed February 3, 2026. <https://www.jstor.org/stable/27672305>.
- Frech, H. E., III, and William C. Lee. 1987. "The Welfare Cost of Rationing-By-Queuing Across Markets: Theory and Estimates from the U. S. Gasoline Crises\*." *The Quarterly Journal of Economics* 102, no. 1 (February): 97–108. ISSN: 0033-5533, accessed April 23, 2025. <https://doi.org/10.2307/1884682>. <https://doi.org/10.2307/1884682>.
- Glaeser, Edward L., and Erzo F. P. Luttmer. 2003. "The Misallocation of Housing under Rent Control." *American Economic Review* 93 (4): 1027–1046. <https://doi.org/10.1257/000282803769206188>.
- Gordon, Robert J. 1973. "The Response of Wages and Prices to the First Two Years of Controls." *Brookings Papers on Economic Activity* 1973 (3): 765–815.
- Grünbaum, Branko. 2003. *Convex Polytopes*. 2nd. Vol. 221. Graduate Texts in Mathematics. New York: Springer.
- Harberger, Arnold C. 1954. "Monopoly and Resource Allocation." *American Economic Review* 44 (2): 77–87.
- Hausman, Jerry A., and Whitney K. Newey. 1995. "Nonparametric Estimation of Exact Consumers Surplus and Deadweight Loss." *Econometrica* 63 (6): 1445–1476.
- . 2016. "Individual Heterogeneity and Average Welfare." *Econometrica* 84 (3): 1225–1248.
- Hughes, Jonathan E., Christopher R. Knittel, and Daniel Sperling. 2008. "Evidence of a Shift in the Short-Run Price Elasticity of Gasoline Demand." *The Energy Journal* 29 (1): 113–134.
- Kang, Zi Yang, and Shoshana Vasserman. 2025. "Robustness Measures for Welfare Analysis" [in en]. *American Economic Review* 115, no. 8 (August): 2449–2487. ISSN: 0002-8282, accessed January 14, 2026. <https://doi.org/10.1257/aer.20220673>. <https://www.aeaweb.org/articles?id=10.1257/aer.20220673>.
- Kholodilin, Konstantin A. 2024. "Rent control effects through the lens of empirical research: An almost complete review of the literature." *Journal of Housing Economics* 63:101976.
- Kominers, Scott Duke, and Piotr Dworczak. 2025. "A Price Theory of Price Gouging."
- Kornai, János. 1992. *The Socialist System: The Political Economy of Communism* [in English]. Princeton, NJ: Princeton University Press. ISBN: 978-0-691-00393-1.
- Kremer, Michael, and Christopher M. Snyder. 2018. *Worst-Case Bounds on R&D and Pricing Distortions*. Working Paper 25119. NBER.

- Murphy, Kevin M., Andrei Shleifer, and Robert W. Vishny. 1992. "The Transition to a Market Economy: Pitfalls of Partial Reform." Publisher: Oxford University Press, *The Quarterly Journal of Economics* 107, no. 3 (August): 889–906. Accessed October 31, 2017. <https://doi.org/10.2307/2118367>.
- Office, Federal Energy. 1974. *Review of Complaints Concerning the Mandatory Petroleum Allocation Program And The Regulation of Petroleum Pricing*. Technical report 090294. <https://www.gao.gov/assets/b-178205-090294.pdf>.
- Oi, Walter Y. 1976. "On Measuring the Impact of Wage-Price Controls: A Critical Appraisal." *Carnegie-Rochester Conference Series on Public Policy* 2:7–64. [https://doi.org/10.1016/S0167-2231\(76\)80003-6](https://doi.org/10.1016/S0167-2231(76)80003-6).
- Poole, Robert W. 1973. "Fuel Shortage: A Prehistory." *Reason*.
- Press, Associated. 1973. "Chicks Smothered as Farmers Decry Price Freeze" [in en-US]. *The New York Times* (June). ISSN: 0362-4331, accessed March 19, 2025. <https://www.nytimes.com/1973/06/27/archives/chicks-smothered-as-farmers-decry-price-freeze.html>.
- Rockoff, Hugh. 1984. *Drastic Measures: A History of Wage and Price Controls in the United States*. New York: Cambridge University Press.
- Smith, Hedrick. 1984. *The Russians* [in en]. Google-Books-ID: LFpbPC2k7NgC. Ballantine Books. ISBN: 978-0-345-31746-9.
- Sowell, Thomas. 1980. *Knowledge and Decisions*. New York: BasicBooks. Reissued 1996.
- TIME. 1973. *CONTROLS: A Threat of Food Shortage* [in en], July. Accessed March 19, 2025. <https://time.com/archive/6841371/controls-a-threat-of-food-shortage/>.
- Times, New York. 1973. "BABY CHICKS KILLED AND COOKED FOR FEED" [in en-US]. *The New York Times* (June). ISSN: 0362-4331, accessed February 1, 2026. <https://www.nytimes.com/1973/06/25/archives/baby-chicks-killed-and-cooked-for-feed.html>.
- U.S. Congress, Joint Economic Committee, Subcommittee on Consumer Economics. 1973. *The gasoline and fuel oil shortage: Hearings before the subcommittee on consumer economics of the joint economic committee, congress of the united states, ninety-third congress, first session, may 1, 2, and june 2, 1973*. Number: 99-740 O tex.entrytype: government. Washington, DC.
- Verleger, Philip K. 1979. "The U.S. Petroleum Crisis of 1979." *Brookings Papers on Economic Activity* 1979 (2): 463–476.
- Weitzman, Martin L. 1977. "Is the Price System or Rationing More Effective in Getting a Commodity to Those Who Need It Most?" *Bell Journal of Economics* 8:517–524.

Yergin, Daniel. 1991. *The prize: the epic quest for oil, money, and power* [in eng]. New York: Simon & Schuster. ISBN: 978-0-671-50248-5.